Chapter 3

Novel aqueous amine blend of 2-(Butylamino)ethanol and 2-Dimethylaminoethanol for CO_2 capture: Equilibrium CO_2 loading, RSM optimization, desorption study, characterization and toxicity assessment

Abstract

This research is necessary to provide a potential aqueous amine blend solvent for industrial application to help in overcoming the challenges of drastic climate change. The performance of a novel aqueous amine blend of 2-(Butylamino)ethanol (BAE) and 2-Dimethylaminoethanol (DMAE) in terms of CO_2 absorption and desorption was investigated. This study focused on aspects such as equilibrium CO_2 loading, absorption capacity, empirical modeling, cyclic equilibrium CO_2 loading, cyclic capacity, heat duty, regeneration efficiency, pH effect, heat of absorption, toxicity assessment, ^{13}C NMR and FTIR speciation, response surface methodology (RSM) modeling, and optimization. The entire CO_2 absorption experiment was performed in the temperature (T) ranging from 298.15–333.15 K, CO_2 partial pressure (P_{CO2}) ranged from 10.13–25.33 kPa, mole fraction of BAE (m_{BAE}) changed from 0.05–0.20, and solution concentration (C) varied from 1–3 mol/L. Desorption experiments were carried out at a constant temperature of 393.15 K and a constant pressure of 25.33 kPa. At T = 313.15 K, P_{CO2} = 25.33 kPa, m_{BAE} = 0.20, and C = 1 mol/L, CO_2 absorption experiments yielded a maximum equilibrium CO_2 loading of

0.9365 mol CO_2/mol amine. At C = 3 mol/L, this novel blend exhibited 71.23 % higher cyclic capacity than conventional 30 wt% Monoethanolamine (MEA). Heat duty and regeneration efficiency of 3 mol/L solution were found to be 112.96 kJ/mol CO_2 and 83.27 %, respectively. This amine blend's heat of CO_2 absorption was determined to be -72.74 kJ/mol. RSM predicted optimum equilibrium CO_2 loading of 0.829265 mol CO_2/mol amine at T = 306.90 K, P_{CO2} = 21.22 kPa, m_{BAE} = 0.16, and C = 1.5 mol/L.

3.1 Introduction

In this contemporary age, the world's population is drastically growing, and to fulfill their basic desires, human beings are wreaking havoc on the earth's climate. Burning fossil fuels due to extensive industrialization releases enormous amounts of carbon dioxide (CO_2) into the environment, leading to drastic climatic changes [1-9]. Global warming is one of the severe issues in the current scenario that is a consequence of the high rate of CO_2 emission in the environment [10-19]. Cement industries, aluminum industries, iron and steel industries, petrochemical industries, thermal power plants, and a variety of other chemical-based industries are the major sectors of high anthropogenic CO_2 emissions [20-24]. Among all these industries, coal-fired thermal power plants contribute massive CO_2 release into the environment and are responsible for one-third of total CO_2 emissions globally [2,7]. According to the Intergovernmental Panel on Climate Change (IPCC) report, if this CO_2 emission rate increases in the same manner and is not checked appropriately, then the earth's temperature will rise by 2 ℃ by the year 2100 [1,25,26]. This scenario would cause sea level rise, flooding, periodic heat waves, drought, the emergence of new viruses such as COVID-19, and other natural disasters, which are the consequences of global warming [13,17,24,27]. In response to all of these dangerous consequences, a

country like India has started working on carbon neutrality and is expected to achieve net-zero emissions by 2070.

The carbon capture and storage (CCS) technique is crucial in combating the adverse effects of global warming [14,21,22,28-31]. There are three main techniques available for CCS: pre-combustion, post-combustion, and oxy-combustion [17,26,27,32]. However, the post-combustion approach is the most established and globally adopted by most industries. It can be retrofitted within the existing operational unit, has a flexible operation, uses less energy, and has a lower operating cost [33]. Methodologies to perform CCS are absorption (mainly via amine scrubbing), adsorption, membrane technology, chemical looping combustion (CLC), cryogenic combustion, and microalgae process [17,20,34,35]. Post-combustion CO_2 capture by amine solvent is the most reliable, highly efficient, and developed method [8,13,16,35-40]. The schematic representation of the various steps involved in implementing the CCS technique is shown in Figure 1.1 of Chapter 1.

For decades, conventional amines such as Monoethanolamine (MEA), Methyldiethanolamine (MDEA), Diethanolamine (DEA), 2-Amino-2-methyl-1-propanol (AMP), and Piperazine (PZ) have been used to capture CO_2 [8,20-22,33,40-42]. Most researchers compared their results with the 30 wt% MEA, which is regarded as the benchmark for most studies [18,30,31,43,44]. Although these amines have good CO_2 absorption performance, but their regeneration energy is very high [31,38,44]. The majority of the literature concluded from experimental analyses that the regeneration energy cost is 70–80 % of the total operational cost [4,11,17,29,35,42]. Due to the limited equilibrium CO_2 loading and high regeneration energy of these amines, the researchers were forced to work on numerous amine blends. Primary or secondary amines, i.e., activators, are blended

with tertiary or hindered amines, i.e., promoters. Activators have a higher heat of absorption ($\Delta H_{abs} \approx 80$ kJ/mol CO_2) than promoters ($\Delta H_{abs} \approx 60$ kJ/mol CO_2), indicating that more energy is required to break down the carbamate products that are formed during CO_2 absorption [1,7,10,16,27,42,45]. Activators have major challenges regarding huge regeneration energy requirements, degradation of equipment, large corrosive behavior, and low absorption capacity [40]. But, the promoters have high CO_2 absorption capacity and low regeneration energy demand [40]. Therefore, blending activators with promoters shows tremendous benefits in terms of the least requirement of regeneration energy demand [13].

2-(Butylamino)ethanol (BAE) is a secondary amine and has steric hindrance with a strong tendency to form bicarbonate on reaction with CO_2 [43]. As a result, equilibrium CO_2 loading can exceed 0.5 mol CO_2/mol amine, resulting in higher cyclic capacity than conventional MEA [24]. In their study, Machida et al. [28] concluded that BAE's hydrophobicity is very high and highly soluble with most amines and ethers. Hydrophobic properties of various amines are mainly responsible for the phase separation of different amine blends in reaction with CO_2. Further, Kim et al. [7] selected six polyamines with high boiling temperature tolerance that can be used for CO_2 capture. Among these polyamines, they selected two polyamines with good cyclic capacity, absorption rate, and considerable heat of reaction. Such polyamines were blended with BAE to balance the inferior properties of these polyamines. Ping et al. [29] prepared non-aqueous solutions of three secondary amines, 2-(Methylamino)ethanol (MAE), BAE, and 2-(Ethylamino)ethanol (EAE) with 2-Butoxyethanol (EGBE) to capture CO_2. The desorption efficiency of these solvents was found in the descending order as BAE > EAE > MAE. The cyclic capacity of non-aqueous BAE was 100 % higher than conventional MEA. BAE/EGBE amine blend has

a low regeneration temperature, an energy-saving solvent. In this series, Dong et al., 2022 [30] calculated CO_2 solubility in the non-aqueous system of BAE blended with EGBE. They concluded that the regeneration energy demand of this amine blend was approximately 1.73 MJ/kg of CO_2, which was 55 % less than the conventional aqueous MEA solution. The advantages of preferring BAE over traditional AMP are that BAE does not produce solid precipitation on CO_2 loading, CO_2 absorption and reaction rate of BAE is higher than AMP, it can be regenerated at low temperature, low heat of CO_2 absorption, and BAE is cheaper than AMP.

2-Dimethylaminoethanol (DMAE) is gaining more attention when selecting tertiary amines since it is produced from renewable resources [40]. DMAE, because of its slightly toxic behavior, makes it very popular due to its negligible environmental hazardous impact. Due to their superb properties, it is replacing most of the existing tertiary amines in the field of CO_2 capture. This tertiary amine is resistant to degradation, has low absorption heat (ΔH_{abs} < 70 kJ/mol), has low regeneration energy demand (83.78 kJ/mol), has a high CO_2 loading capacity and low viscosity [9,16,40]. Chowdhury et al. [10] concluded that DMAE has a much higher CO_2 absorption capacity than traditional MDEA. Hadri et al. [33], in their investigation, concluded that the equilibrium CO_2 loading of MDEA is lower than that of DMAE at 30 wt% solution concentration, 40 ℃ temperature, 1 atmospheric bar pressure, and 15 % CO_2 concentration in the flue gas stream. As a result, the individual advantages of BAE and DMAE can be utilized by blending them. The BAE+DMAE novel amine blend would perform well in absorption rate, cyclic capacity, and regeneration energy demand.

As CO_2 underwent a chemical reaction with the amine blend of BAE+DMAE, new species were formed. These species were the intermediate complexes of BAE, DMAE, and

bicarbonate or carbonate. Their authentication can be accomplished using the Fourier transform infrared spectroscopy (FTIR) and ^{13}C nuclear magnetic resonance spectroscopy (NMR) characterization techniques [1,15,16,29,31,44,46]. Equilibrium CO_2-loaded amine blend solutions were utilized for the calculation of heat duty and regeneration efficiency during the desorption experiments [13,34,39,47]. Assessment of the toxicity level of BAE and DMAE was very essential from the environmental point of view; therefore, it was judged in terms of lethal dose (LD_{50}), and toxicity was defined in four different categories [48,49]. In the current scenario, optimization through response surface methodology (RSM) software is becoming very popular in the research field. RSM is a credible chemometric method that is used to predict many variables involved in the system [50]. Based on the operating range, RSM designs the experimental runs, develops a model equation, and ultimately optimizes the results [51-55]. Equation modeling is most commonly based on quadratic equations due to their highly trusted results and the inclusion of the entire factors for any specific system. There are several designing tools available for optimization, but the Central composite design (CCD) and box-behnken design (BBD) are very popular. In most of the experimental work, CCD has been used for the optimization task [50,53,55-59]. However, BBD's optimization approach is highly acceptable, and it requires the fewest number of experimental runs when the number of independent variables is large [60]. BBD design was adopted by Amiri et al. [54], Nuchitprasittichai et al. [61], Sahraei et al. [60], and Nuchitprasittichai et al. [62] to optimize their desired parameter. To examine the significance of the model, analysis of variance (ANOVA) plays a significant role, and the values of degree of freedom (df), F-value, p-value, and lack-of-fit are mainly focused [58,59].

In this work, a novel BAE+DMAE amine blend was selected to investigate CO_2 absorption and desorption behavior. Toxicity assessment of BAE and DMAE, along with other major amines, was studied to categorize them in terms of adverse environmental impacts. Four important parameters of temperature (T), CO_2 partial pressure (P_{CO2}), mole fraction of activator, BAE (m_{BAE}), and solution concentration (C) were chosen for analyzing their individual effects on equilibrium CO_2 loading. The study of intermediate complexes so formed during CO_2 absorption in the novel aqueous amine was investigated by adopting FTIR and NMR techniques. A semi-empirical model was developed to validate the experimental results. The desorption study calculated cyclic equilibrium CO_2 loading, cyclic capacity, heat duty, and regeneration efficiency at specific operating conditions. Finally, the response surface methodology (RSM) software benefitted in providing the optimized value of equilibrium CO_2 loading along with various other parameters involved in the entire system. RSM software developed a model equation, and this RSM modeling predicted the output and finally validated the entire experimental work.

Novelty of the present experimental work:

1. A very least work on BAE and DMAE has been carried out to capture CO_2; therefore, the aqueous amine blend of BAE + DMAE is unique and entirely novel.

2. DMAE can be produced from renewable resources, and BAE is less expensive than traditional AMP, so the overall cost of this novel amine blend can be reduced to a large extent.

3. This novel amine blend exhibited marvelous CO_2 absorption performance, and its equilibrium CO_2 loading was higher than most amine blends, as reported in most of the literature.

4. Solid precipitation on CO_2 loading causes fouling in the pipeline of the operational industries, which is the biggest concern of most of the aqueous traditional amine blends. However, according to experimental results, the BAE+DMAE amine blend is not corrosive in nature.

5. This unique amine blend's FTIR and ^{13}C NMR spectroscopic analysis had never been reported before; however, the current work covered all such characterizations.

6. This novel amine blend has shown promising results in heat duty, regeneration efficiency, cyclic capacity, and heat of CO_2 absorption as compared with 30 wt% traditional MEA.

7. The toxicity of this novel amine blend is slightly toxic, which is one of the novelties of the present experimental work since most of the reported amine blends are highly toxic, leading to adverse environmental effects.

8. Finally, the RSM software approach for optimization of equilibrium CO_2 loading and RSM modeling is very rare, but they were also incorporated in this work.

3.2 Experimental section

3.2.1 Chemicals and instruments used

The BAE (purity ≥ 98 %) and DMAE (purity ≥ 98 %) amine chemicals were procured from Sigma-Aldrich, U.S.A, and Sisco Research Laboratories, New Mumbai, India, respectively. The amine blend of BAE and DMAE of different compositions was used for the experiments under various operating conditions. MEA, purity ≥ 98 % was purchased from Sd fine chemical, India, and it was used as a benchmark for validating the experimental setup and comparing the experimental results. Hydrochloric acid (HCL, purity = 35-38 %) was acquired from Merck, Germany, and its 1 M HCL solution was used

for titration to estimate equilibrium CO_2 loading. Dimethyl sulfoxide-d_6 (DMSO-d_6, 99.9 atom % D) was purchased from Sigma-Aldrich and used as a signal lock during NMR analyses. Descriptions of all the chemicals, along with their important properties are listed in Table 3.1. Pure nitrogen (N_2) and CO_2 gas cylinders were supplied by Linde India Limited, India. A digital mass flow controller was provided by Alicat Scientific, India (Model No:- MC-500SCCM-D-DB9M, $\pm$ 0.32 % reading or $\pm$ 0.02 % full scale). United Phosphorus Limited, Mumbai, India, supplied a portable infrared CO_2 gas analyzer (Sr. no. A-191 (PM), Gasboard-3800P, software version–1606.25, CO_2 analysis range- 0–100 % V/V). A digital pH meter (Model: CL-54+, Sr. No: 20K1595) to measure the pH of CO_2-unloaded, CO_2-loaded, and CO_2-regenerated amine blend samples was acquired from Toshniwal Instruments Mfg. Pvt. Ltd., Ajmer, India. Double distilled water was prepared on the lab scale for sample preparation during the entire experimental work.

Table 3.1 Specification and entire properties of all the chemicals used in the experimental work.

Chemicals	Structure	CAS Number	Molecular weight (g/mol)	BP (℃)	ρ (Kg/m^3)	Initial purity	Analysis method	Supplier	Purification method
2-(Butylamino)ethanol (BAE)	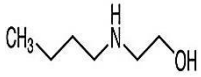	111-75-1	117.19	198-200	891	≥ 98%	Gas-chromatography (GC-Analysis)	Sigma-Aldrich, U.S.A	None
2-Dimethylaminoethanol (DMAE)	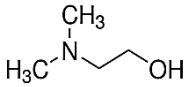	108-01-0	89.138	134.1	890	≥ 98%	Gas-chromatography (GC-Analysis)	SRL Private limited, India	None
Monoethanolamine (MEA)	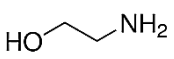	141-43-5	61.08	170	1011.7	≥ 98%	Gas-chromatography (GC-Analysis)	Sd Fine chemical limited, India	None
Hydrochloric acid (HCL)	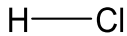	7647-01-0	36.46	-85.05	1200	35-38%	-	Merck, Germany	None
Carbon dioxide gas (CO_2)	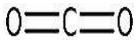	124-38-9	44.01	-78.46	1.98	99.99%	-	Linde India limited	None
Nitrogen gas (N_2)	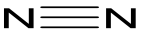	7727-37-9	14.00	-195.8	1.25	99.99%	-	Linde India limited	None
Dimethyl sulfoxide-d_6 $(CD_3)_2SO$	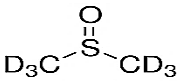	2206-27-1	84.17	189	1190	99.9%	Gas-chromatography (GC-Analysis)	Merk, Germany	None
Distilled Water (H_2O)		7732-18-5	18.02	100	998.2	99.9%	-	Prepared at lab scale	Double distillation

3.2.2 Analytical techniques for characterization

The novel aqueous amine blend of BAE+DMAE of the desired composition was prepared with double distilled water. The CO_2 absorption and desorption experiments were conducted to obtain the CO_2-loaded and CO_2-regenerated amine blend samples. Now, these CO_2-unloaded, CO_2-loaded, and CO_2-regenerated samples were characterized by adopting FTIR and ^{13}C NMR techniques. The FTIR spectrophotometer instrument with the KBr sampling technique benefitted in detecting chemical species present in the novel amine blend. The characteristic peaks so obtained were helpful in analyzing the functional groups of specific compounds.

Similarly, ^{13}C NMR tests were conducted by NMR spectrometer instrument, and Tetramethylsilane ($(CH_3)_4Si$) was used as an internal reference with a chemical shift of 0.00 ppm. DMSO-d_6 was added to each amine blend sample before performing an NMR investigation. This spectroscopic method also authenticated the occurrence of chemical reactions of CO_2 with the novel aqueous amine blend. This NMR test has also evaluated the chemical compounds present in the CO_2-unloaded, CO_2-loaded, and CO_2-regenerated amine blend samples. The detailed information on FTIR and ^{13}C NMR investigation has been incorporated further in sections 3.3.2 and 3.3.3, respectively.

3.2.3 Description of the CO_2 absorption setup

The CO_2 absorption experimental setup can be divided into three major categories: (a) preparation of simulated flue gas stream composed of CO_2 and N_2 gases, (b) CO_2 gas absorption in the aqueous amine blend, and (C) analysis of flue gas composition coming out from the amine blend. The complete diagrammatic representation of CO_2 absorption setup is shown in Figure 3.1. 46.7 L capacity and 99.99 % purity of CO_2 and N_2 gas

cylinders were used to prepare the simulated CO_2 flue gas stream on the lab scale. The presence of an on-off valve and pressure gauge indicators (in bar/psi) on the cylinders aided in the extraction of gases from each cylinder. Each of the gases was routed through the digitally operated mass flow controllers. These controllers precisely controlled the flow rate of each of the gases. A proper fixed total flow rate of the simulated CO_2 flue gas stream was maintained for the entire experimental task. Based on the CO_2 and N_2 gas flow rate, a certain mole percent of CO_2 was available for every different run set. CO_2 and N_2 gases were then passed through the mixing chamber and the helical gas mixing coils to ensure proper gas mixing. The flue gas stream was then directed towards the CO_2 gas analyzer to ensure that the required mole percent of CO_2 in the flue gas stream was obtained. The flue gas stream was introduced into the gas dispenser, creating the wet gaseous mixture of the simulated flue gas. Afterward, this stream was sent to the bubble column reactor.

A digital temperature-controlled water bath (Jindal, S.M. Industries Delhi, India) provided the required heating temperature. This water bath had a shaker with a speed regulator that provided a uniform temperature inside the water bath. A thermometer was used at regular intervals to cross-check the water bath temperature. The CO_2 absorption task was carried out in a glass-based borosilicate bubble column reactor with dimensions of 35.5 cm in length, 3 cm in diameter, and a volume capacity of 150 ml. A known composition of an aqueous amine blend of BAE and DMAE was poured inside the bubble column reactor for further experimental work. The simulated flue gas interacted with the amine blend solution within the reactor and was absorbed over time (semi-batch operation). The outlet stream of the bubble column reactor was condensed before being routed to the

silica gel bed for moisture removal. Ultimately, this dry stream was connected to the CO_2 gas analyzer, which indicated the degree of CO_2 saturation of the solution.

3.2.4 CO_2 absorption experiment

All the experiments were performed at T = 298.15–333.15 K, P_{CO_2} = 10.13–25.33 kPa, m_{BAE} = 0.05–0.20, C = 1–3 mol/L, and absorption time (θ) = 10 hours (Complete saturation). T, P_{CO_2}, m_{BAE}, C and θ are five independent variables on which the experimental equilibrium CO_2 loading depends (α_{exp}). It can be represented as α_{exp}= function (T, P_{CO_2}, m_{BAE}, C and θ). A manual run sheet comprised of experimental run sets was created corresponding to the above-mentioned independent variables at various operating conditions. The separate experimental run sets were also obtained from the design expert software of trial version 8.0.6, and the equilibrium CO_2 loading was examined in the above aforementioned operating conditions.

The known composition of the simulated CO_2 flue gas stream coming out from the helical mixing coil was connected to the portable CO_2 gas analyzer. This infrared-based gas analyzer measures the CO_2 gas composition in volume % [15,34]. After waiting for a certain time (in min.), the known composition of CO_2 in the flue gas stream was attained and digitally authenticated by the CO_2 gas analyzer. This indicated that the flue gas stream was then ready to be used for absorption. 100 ml of known concentration of the novel aqueous amine blend of BAE+DMAE was prepared from the double distilled water and poured inside the bubble column reactor. This bubble column reactor was placed inside the temperature-controlled water bath and this water bath exhibited a commendable accuracy of $\pm$ 1 K. The incubator shaker, thermocouple, and heating indicator were present in the water bath, and they were helpful in achieving the desired temperature. The water bath

temperature was monitored externally using a thermometer with 0.1 K sub-divisions [20-22]. The simulated CO_2 flue gas stream was absorbed in the aqueous amine blend of BAE+DMAE under different operating conditions. All the absorption experiments were conducted at 1 atmospheric pressure. The total flow rate of the simulated flue gas stream was 240 ml/min used for the entire experiment [5,8,22,25,26,34,47]. The lab-scale simulated flue gas stream was passed through this amine blend for absorption. At a periodic interval of every 10 minutes, the gas stream coming out from the aqueous amine blend was continuously analyzed. The complete schematic representation of the absorption setup is shown in Figure 3.1. The CO_2 saturation level of the amine blend solution was determined by a CO_2 gas analyzer and is expressed in volume percentage. The chemical reactions initiated CO_2 gas absorption in the aqueous amine blend. This phenomenon is called 'CO_2 loading', which is defined as the number of moles of CO_2 dissolved per mole of amine solvent used. At complete CO_2 saturation of the amine blend, it is technically termed 'equilibrium CO_2 loading'.

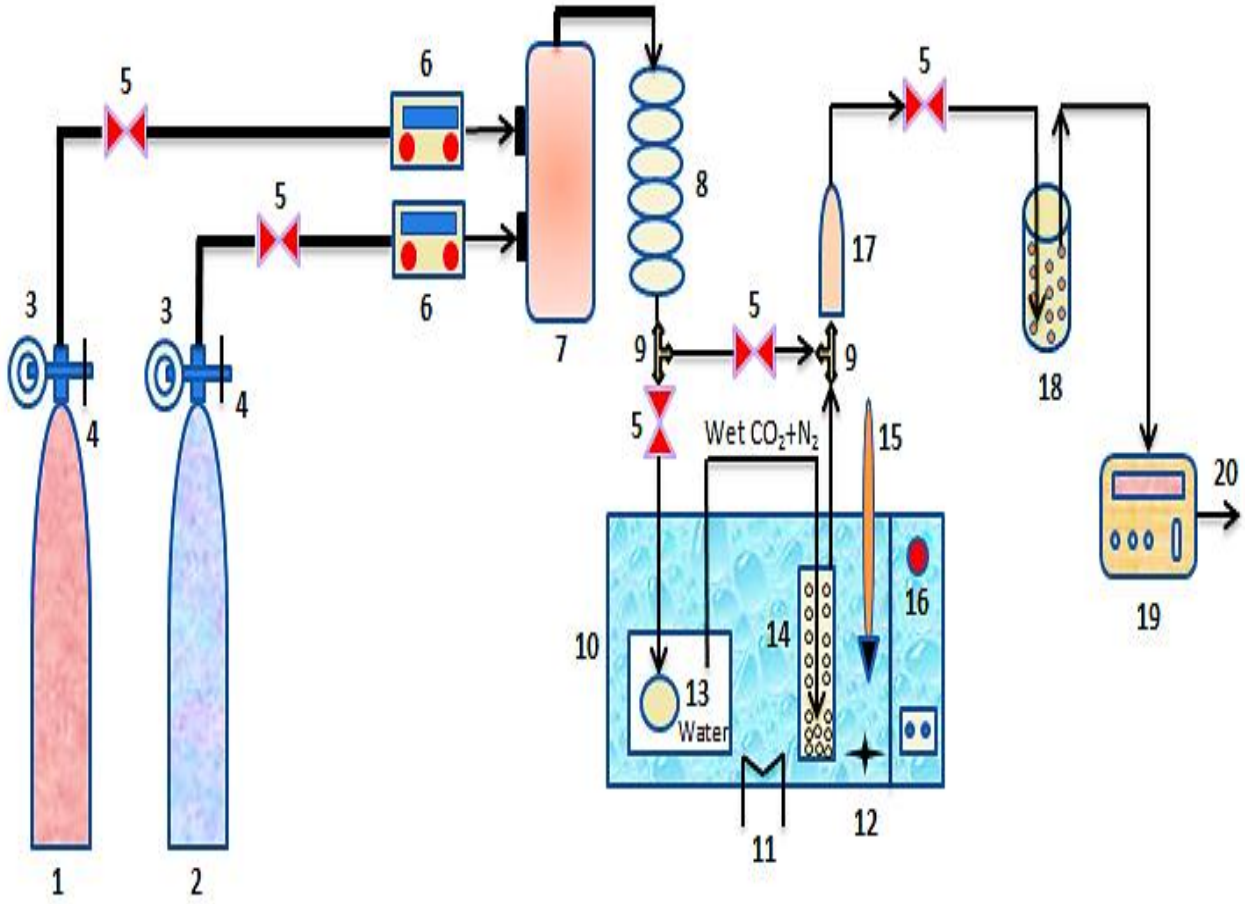

Figure 3.1 The complete diagrammatic representation of the absorption setup used to perform absorption experiments for the novel aqueous amine blend of BAE+DMAE, (1) CO_2 gas cylinder; (2) N_2 gas cylinder; (3) Pressure indicator; (4) Pressure regulator; (5) Control valve; (6) Digital mass flow controller; (7) Gas mixing chamber; (8) Gas mixing coils; (9) T-joint; (10) Water bath with thermocouple; (11) Heating medium; (12) Agitator; (13) Gas disperser; (14) Bubble column reactor; (15) Thermometer; (16) Power indicator of water bath; (17) Condenser; (18) Silica bed for moisture removal; (19) Portable infrared CO_2 gas analyzer; (20) Outlet stream.

The experiments were halted when the analyzer displayed the constant known composition at the inlet and outlet, indicating that the amine blend solution was completely CO_2-saturated. The equilibrium CO_2 loading (mol CO_2/mol amine) can be determined experimentally using the Chittick apparatus [4,5,15,24,31,34,38,47]. 1 ml of CO_2 saturated amine blend sample was extracted from the bubble column reactor and titrated with 1 molar HCL stock solution. Adding a few drops of methyl orange (CDH private limited, New Delhi, India) as an indicator in the CO_2-saturated amine sample, the ultimate endpoint of the titration was determined. Each titration experiment was repeated three times to ensure accuracy, and the average value was finally reported. The amount of CO_2 dissolved in the amine blend can be calculated by the water displaced during titration. The volumetric method is helpful in estimating the equilibrium CO_2 loading (Eq. 3.1) [5,8,25,22]. The error bar for each experimental data point corresponding to equilibrium CO_2 loading was found to be $\pm$ 0.02 mol CO_2/mol amine. This error bar was mainly due to a variation of $\pm$ 0.5 ml of water collected during the titration.

The calculation of equilibrium CO_2 loading (α) was done by using the correlation as provided in our previous work [1], which is as follows:

$$\alpha = 12.1942 \times \frac{V_{CO_2}}{C_{blend} \times V_{CO_2\ saturated}} \times \frac{1}{(273.15+T)} \text{ ; mol } CO_2\text{/mol amine} \quad (3.1)$$

$$\text{Absorption capacity} = \alpha . C_{blend} \text{ ; mol } CO_2\text{/L. solution} \quad (3.2)$$

Where α denotes equilibrium CO_2 loading and V_{CO_2}, C_{blend}, $V_{CO_2\ saturated}$, T are the volume of CO_2 gas released (in L) from the amine solution, amine blend concentration (in mol/L), volume of CO_2 saturated amine sample (in L), and room temperature (in ℃), respectively.

3.2.5 Description and investigation of CO_2 desorption setup

The equilibrium CO_2-loaded amine samples were collected from the bubble column reactor to study the desorption behavior of the aqueous amine blend of BAE+DMAE. Initially, desorption experiments were carried out in a three-necked round bottom flask (desorption reactor) composed of borosilicate glass [5,8,12,47]. This flask has a volume capacity of 500 ml, and the 60 ml CO_2-saturated amine blend samples were poured from one of its necks. The CO_2-loaded amine temperature inside the desorption reactor was measured using an analog thermometer inserted through the second neck, and the last neck was connected to the condenser. Two necks of the flask were closed with the cork, and the third one was associated with the condenser. The desorption reactor was placed on a glass insulator filled with viscous and colorless silicon oil (Central Drug House Private Limited, India). The desorption heat was constantly provided to the glass insulator by an electric hot plate (IKA®, India Private Limited, India; Model no. IKA® C-MAG HS 7; Accuracy: $\pm$ 10 K). This digital temperature-controlled heating plate apparatus with a magnetic stirrer heated the silicon oil. The oil bath temperature was raised to 393.15 K, and 60 ml of the CO_2-loaded amine blend samples were immersed in the desorption reactor for further procedure. A thermocouple sensor (IKA®, India Private Limited, India; Model no.: ETS-D5, 8–16V, 15mA) was immersed directly in silicon oil to accurately measure its temperature [24]. The complete representation of the desorption setup for the regeneration of the CO_2-loaded amine blend sample has been shown in Figure 3.2. It closely resembles the configuration found in the majority of the literature [8,12,15,22-24,29,47,34]. Keeping the amine blend sample at a constant temperature of 393.15 K inside the desorption reactor was challenging. Minor temperature fluctuation hindered this amine blend from attaining

this constant temperature. So, the fixed desorption temperature was attained within a $\pm$ 5 K error, as reported by the thermometer. A magnetic bead at the bottom of the desorption reactor provided the uniform mixing of the amine blend samples stirred at 500 rpm [15].

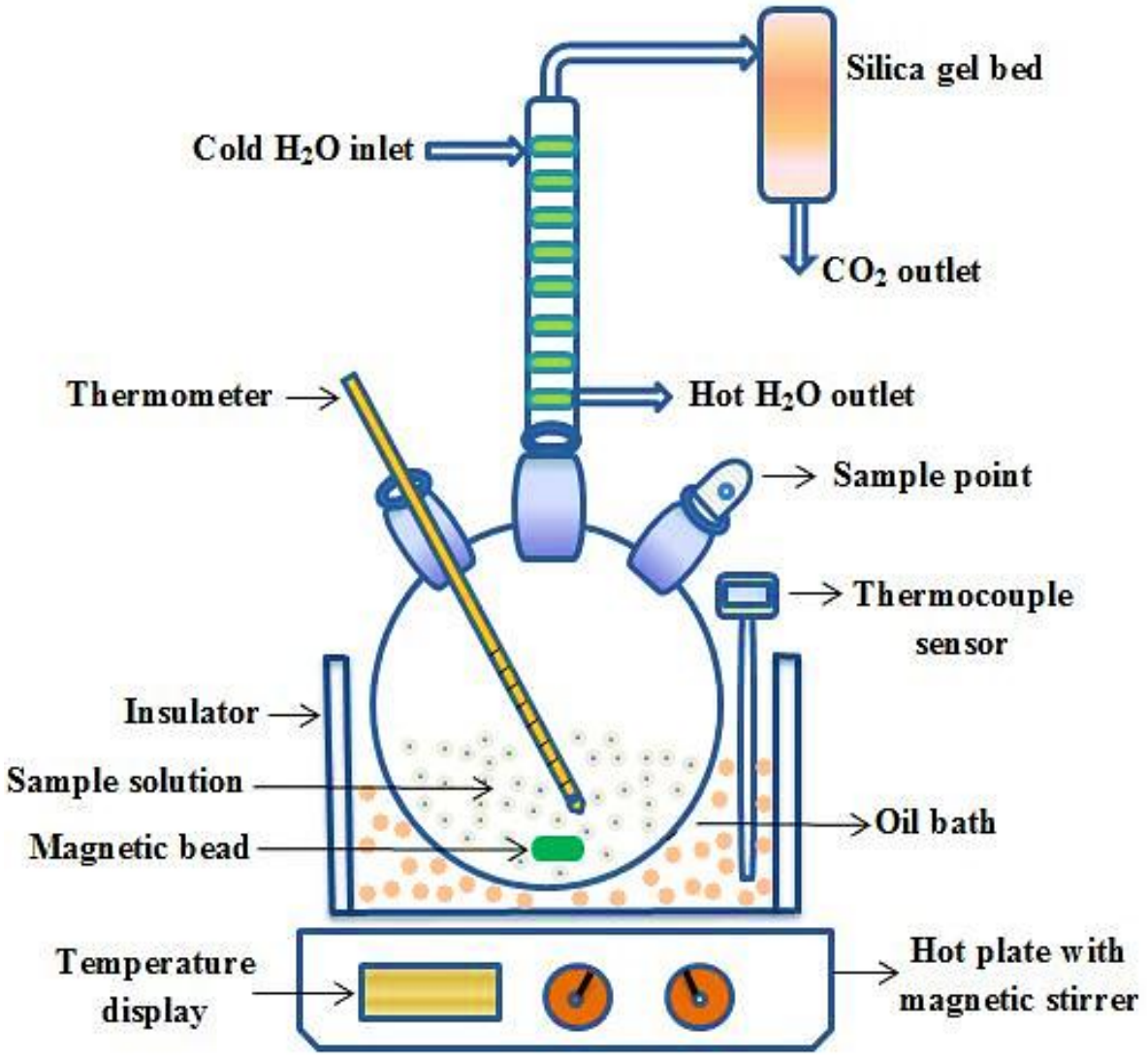

Figure 3.2 The schematic representation of desorption setup used to perform desorption experiments for the novel aqueous amine blend of BAE+DMAE.

Cooling water was circulated at 293 K through the condenser attached to one of the desorption reactor's necks. The condenser benefitted in preventing the amine and water vaporization losses [5,7,22-24,34]. The oil bath at 393.15 K and the CO_2-saturated amine in the desorption flask reached thermal equilibrium in about 10–15 minutes. After this situation, at the fixed interval of every 5 minutes, the CO_2 loading was calculated by the Chittick apparatus. This procedure was continued till the constant equilibrium CO_2 loading was attained. Cyclic equilibrium CO_2 loading and cyclic capacity were calculated by using Eq. (3.3) and Eq. (3.4), respectively.

$$\Delta\alpha = \alpha_{313.15k,25.33kPa} - \alpha_{393.15k,25.33kPa} \text{ ; mol } CO_2\text{/mol amine} \quad (3.3)$$

$$\text{Cylic capacity} = \Delta\alpha . C_{blend} \text{ ; mol } CO_2\text{/L solution} \quad (3.4)$$

3.2.6 Heat duty and regeneration efficiency calculation

The value of heat duty can be achieved by determining the value of steady-state heat transfer from the silicon oil to the desorption flask and the amount of CO_2 removed while regenerating the CO_2-saturated amine blend samples. Fourier's correlation (Eq. 3.5) provided the value of heat transfer, which is represented as follows:

$$q = \frac{KAdT}{dx} \text{ ; J/s} \quad (3.5)$$

Where q is the heat transfer rate in the steady state (J/s); K is the thermal conductivity of the desorption reactor made up of Pyrex glass material ($\frac{W}{m-K}$); A is the surface area of amine solution (spherical sector) filled inside the desorption reactor (m^2); dT is the temperature difference between silicon oil bath and the amine blend sample (K); dx is the thickness of the desorption reactor (m).

The amount of CO_2 removed can be calculated by the cyclic capacity of the amine blend, and it is correlated as:

$$CO_2 \text{ removed } = \frac{\Delta\alpha \times C_{blend} \times V}{t} \text{; mol } CO_2/s \quad (3.6)$$

Where $\Delta\alpha . C_{blend}$ is the cyclic capacity (mol CO_2/L Solution); V is the volume of aqueous amine blend solution (ltr.); t is the desorption time (sec.). For this present work, the desorption experiments were performed for a fixed time period of 30 minutes.

The final expression of heat duty based on Eq. 3.5 and Eq. 3.6 is as follows:

$$Q_{Reg} = \frac{q}{CO_2 \text{ removed}} \text{; kJ/mol } CO_2 \quad (3.7)$$

Muchan et al. [13] and Narku-Tetteh et al. [47] provided a similar correlation for estimating heat duty in their studies.

$$\text{Efficiency of regeneration } (\%) = \left(\frac{\text{Cyclic capacity}}{\text{Absorption capacity}}\right) \times 100 \quad (3.8)$$

3.2.7 Study of heat of CO_2 absorption (ΔH_{abs})

When CO_2 gets absorbed in any aqueous amine blend, it liberates some heat, which is referred to as heat of CO_2 absorption. It is well evident from previous studies that the regeneration cost is approximately 70–80 % of the entire operational cost [1]. In this chain, the heat of CO_2 absorption plays a vital role in providing information regarding regeneration heat and its cost-effectiveness for the chosen aqueous amine blend. The activators are classified under high kinetics solvents because of the high value of heat of CO_2 absorption ($\Delta H_{abs} \approx 80$ kJ/mol CO_2). The promoters are placed under low kinetics solvents due to their low value of heat of CO_2 absorption ($\Delta H_{abs} \approx 60$ kJ/mol CO_2) [45]. Activators and promoters provide maximum equilibrium CO_2 loading up to 0.5 and 1 mol CO_2/mol amine, respectively [1,26]. Activators produce carbamate when reacting with CO_2, but promoters do not because there is no hydrogen atom connected with the nitrogen atom in tertiary amine [13,45,26].

The value of ΔH_{abs} can be calculated from the solubility data, and it is also the function of T and P_{CO2}. The CO_2 solubility of the present aqueous amine blend of BAE+DMAE was calculated at temperatures ranging from 298.15 to 333.15 K, while the partial pressure of CO_2 for this system varied from 10.13 to 25.33 kPa. The heat of CO_2 absorption can be calculated with the help of the Gibbs-Helmholtz equation [17,43,44], and it is represented by Eq. 3.9 as:

$$\frac{d[\ln(P_{CO2})]}{d(\frac{1}{T})} = \frac{\Delta H_{abs}}{R} \tag{3.9}$$

Where $P_{CO2,}$T, ΔH_{abs}, and R represents the CO_2 partial pressure (kPa), working temperature (K), heat of CO_2 absorption (J/mol), and universal gas constant [J/(mol.K)], respectively. The product of slope plotted in between $\ln(P_{CO2})$ vs. $(\frac{1}{T})$ by R provides the value of ΔH_{abs}. For nearly similar equilibrium CO_2 loading, several data sets of P_{CO2} and $(\frac{1}{T})$ were chosen for the estimation of the heat of CO_2 absorption. Most researchers rely on the Gibbs-Helmholtz equation for the estimation of ΔH_{abs} value, and this was found in the majority of the literature [8,32,63-65].

3.2.8 pH measurement of amine blend

Toshniwal Instruments Mfg. Pvt. Ltd., Ajmer, India, provided a digital pH meter with model number CL-54+, serial number 20K1595, and an accuracy of $\pm$ 0.01 pH. This instrument was used to determine the pH of all solutions, including CO_2-unloaded, CO_2-loaded, and CO_2-regenerated amine blend samples. The pH instrument was calibrated with the help of standard buffer solutions of 4, 7, and 9.18. All these buffer solutions were purchased from Fischer Scientific. Measuring the pH of the aqueous amine blend of

BAE+DMAE is vital since it shows the amount of CO_2 absorbed in different amine blend solutions.

3.2.9 Designing of experiments

RSM is a statistical approach for the optimization of challenging problems due to more efficient and simple arrangements of the experiments. Designing various experimental run sets was prepared with the help of the Design-Expert® software of trial version 8.0.6. Temperature (T = 298.15–333.15 K), partial pressure of CO_2 (P_{CO2} = 10.13–25.33 kPa), mole fraction of activator, BAE (m_{BAE} = 0.05–0.20), and solution concentration (C = 1–3 mol/L) were the four independent variables (i.e., numeric factors) involved in this work that has been input in the software. Design expert software provided an overall 30 experimental runs with 6 center points and 24 non-center points. The equilibrium CO_2 loading was the only response to this entire experimental work. There are many designing tools available for the optimization of any engineering problem, and they are CCD, BBD, one-factor design, optimal design, user-defined design, historical data design, 3-level factorial design, and so on [1]. For this present work, CCD was selected to optimize the equilibrium CO_2 loading as a final response. Each numeric factor is varied on five levels: plus and minus alpha (axial points), plus and minus 1 (factorial point), and central points. Various run sets with different operating conditions were achieved after successfully inputting the numeric factors in the RSM software. ANOVA with a lack-of-fit test was examined to validate the experimental results and fitness of the chosen model.

3.2.10 Toxicity assessment

Investigation of the toxicity level of amines is very crucial to assess due to their adverse impacts on the environment and human health. Toxicological information on various

amines can be obtained by considering the lethal dose (LD_{50}) information provided in the material safety data sheet (MSDS). LD_{50} is the quantity of chemical required that causes death in 50 % of the animal population present in a group, and it is measured in mg/Kg [48]. Based on the hazardousness of the chemicals, the Environmental protection agency (EPA) has categorized various chemicals into four major categories. Information regarding the classification of amines, LD_{50} range, and toxicity level is shown in Table 3.2.

Table 3.2 Classification of different amines and their toxicity level based on LD_{50} range [49].

Amine classification	**LD_{50} range (mg/kg)**	**Toxicity level**
Category 1st	$LD_{50} \leq 50$	Highly toxic
Category 2nd	$50 < LD_{50} \leq 500$	Moderately toxic
Category 3rd	$500 < LD_{50} \leq 5000$	Slightly toxic
Category 4th	$LD_{50} > 5000$	Safe to use

Category 1st: when any chemical has $LD_{50} \leq 50$ mg/Kg, then it is highly toxic in nature; Category 2nd: $50 < LD_{50} \leq 500$ mg/kg, it is classified under moderately toxic chemicals; Category 3rd: $500 < LD_{50} \leq 5000$ mg/kg, it is classified under slightly toxic chemicals and Category 4th: $LD_{50} > 5000$ mg/kg, these chemicals are very safe to use [49]. When capturing CO_2 with various aqueous amines, it is critical to select amines that have low environmental and human health risks. Therefore, amines with high toxicity levels and a high probability of forming toxic degradable products are not a good choice for CO_2

capture. In this chain, amines that are classified under categories 1st and 2nd are never recommended to be used for CO_2 capturing purposes.

3.3 Reaction mechanism and characterization

3.3.1 Reaction chemistry of the amine blend system (BAE + DMAE + H_2O + CO_2)

When amines react with CO_2, three mechanisms exist: zwitterion mechanism, ter-molecular mechanism, and base-catalyzed hydration mechanism. Most of the researchers adopted the zwitterion mechanism for the aqueous alkanolamine solvents. Caplow [66] discovered this mechanism in 1968, and further, this mechanism was modified by Danckwerts [67] in 1979. In this mechanism, various classifications of amines, like primary amine, secondary amine, and hindered amine, react with CO_2 to form a zwitterion complex [17]. This complex is deprotonated to form carbamate with the assistance of the second amine molecule (i.e., base; B) [11,12,15]. It was discovered that tertiary amines do not directly react with CO_2 but rather act as a base catalyst that promotes CO_2 hydration [11], and Donaldson and Nguyen [68] validated this concept. These reactions are as follows:

Zwitterion formation step: $CO_2\ (aq.) + R_1R_2NH \leftrightarrow R_1R_2NH^+COO^-$ (3.10)

Deprotonated step: $R_1R_2NH^+COO^- + B \leftrightarrow R_1R_2NCOO^- + BH^+$ (3.11)

The aqueous amine blend of BAE+DMAE in reaction with CO_2 gives a set of chemical reactions. These reactions involve the solubility of CO_2 in the aqueous phase, H_2O dissociation, bicarbonate/carbonate ion formation, and BAE/DMAE intermediate reactions. ^{13}C NMR and FTIR spectroscopic analyses were helpful in determining and authenticating the chemical species available in the entire system. The set of all the chemical reactions is as follows:

Physical CO_2 solubility:

$$CO_2\ (g) \overset{H_{CO_2}}{\longleftrightarrow} CO_2\ (aq.) \quad (3.12)$$

Dissociation of H_2O molecule:

$$H_2O \overset{K1}{\leftrightarrow} H^+ + OH^- \quad (3.13)$$

Bicarbonate ion formation [9**]:**

$$CO_2 + H_2O \overset{K2}{\leftrightarrow} HCO_3^- + H^+ \quad (3.14)$$

$$CO_2 + OH^- \overset{K3}{\leftrightarrow} HCO_3^- \quad (3.15)$$

Carbonate ion formation:

$$HCO_3^- \overset{K4}{\leftrightarrow} CO_3^{2-} + H^+ \quad (3.16)$$

DMAE intermediate reactions [1,40,41**]:**

$$DMAE + H^+ \overset{K5}{\leftrightarrow} DMAEH^+ \text{ (Protonation of DMAE)} \quad (3.17)$$

$$CO_2 + DMAE + H_2O \overset{K6}{\leftrightarrow} DMAEH^+ + HCO_3^- \quad (3.18)$$

BAE intermediate reactions [38**]:**

$$BAE + CO_2 \overset{K7}{\leftrightarrow} BAE^+COO^- \quad (3.19)$$

$$BAE + BAE^+COO^- \overset{K8}{\leftrightarrow} BAEH^+ + BAECOO^- \quad (3.20)$$

$$BAECOO^- + H_2O \overset{K9}{\leftrightarrow} HCO_3^- + BAE \quad (3.21)$$

$$BAE + CO_2 + H_2O \overset{K10}{\longleftrightarrow} HCO_3^- + BAEH^+ \quad (3.22)$$

Overall reaction of the entire system:

$$2BAE + 3DMAE + 4CO_2 + 4H_2O \overset{K11}{\longleftrightarrow} 3HCO_3^- + CO_3^{2-} + 2BAEH^+ + 3DMAEH^+$$

(3.23)

H_{CO_2} is the 'Henry's constant'; Eq. 3.12 to Eq. 3.23 represents the number of chemical reactions involved in the entire aqueous amine blend system; K1–K11 is the chemical reaction equilibrium.

3.3.2 Fourier transform infrared spectroscopy (FTIR analysis)

FTIR test was helpful in detecting the functional groups of all the chemical species available in any sample in the form of different peaks within the specified spectrum range [15,29,31]. FTIR analysis was performed with the help of an FTIR spectrophotometer instrument (Model: Nicolet iS5; Company: THERMO Electron Scientific Instruments LLC, USA). The KBr pellet sampling technique was used to record infrared spectra lying in the range of 4000–400 cm^{-1}. The resolutions were recorded at 4 cm^{-1}, and the number of scans was 32. The functional groups of CO_2-unloaded, CO_2-loaded, and CO_2-regenerated amine blend samples were examined by the FTIR technique. For this work, the FTIR analyses of various samples were correlated between transmittance (in %) and the wavenumber (in cm^{-1}).

3.3.3 Nuclear magnetic resonance spectroscopy (NMR analysis)

NMR technique is a terrific non-invasive analytical method for detecting the chemical species present in any sample that contains nuclei having a magnetic moment [1,16,44,46]. The three isotopic methods for obtaining the relative peaks of any chemical species while performing NMR spectroscopy are ^{1}H, ^{13}C, and ^{15}N [69]. As previously reported in section 3.2.2, the species available in the CO_2-unloaded, CO_2-loaded, and CO_2-regenerated amine blend samples were checked and authenticated using this technique. The NMR tests were carried out using an OneBay NMR spectrometer instrument (Model: AVH D 500 AVANCE III HD 500 MHz; Company: BRUKER BioSpin INTERNATIONAL AG). 0.6

ml of each amine blend sample was taken in the NMR tubes and characterized by adopting the ^{13}C NMR spectroscopy at room temperature [1,14,18]. To provide good signaling, DMSO-d_6 has been used as a deuterium lock, and 0.3 ml of its dose was added to each amine blend sample. Tetramethylsilane ((CH3)4Si) was used as an internal reference throughout the entire experiment. Parameters involved in the ^{13}C NMR analysis were the operating spectral frequency = 125.8131145 MHz, time delay = 2 s, spectral width = 29761.904 Hz, total no. of scans = 256, and acquisition time = 1.101 s.

3.4 Results and discussion

3.4.1 Experimental setup validation

Before performing actual experiments, it was mandatory to validate the experimental setup, so to attain this task, a conventional 30 wt% MEA solution was considered as a benchmark. Experimental results were validated by comparing them with the equilibrium CO_2 loading as found in most of the literature [15,36,70-73]. Such setup validation experiments were performed at a constant temperature (T) of 313.15 K, and different values of CO_2 partial pressure (P_{CO2}), i.e., 2.2 kPa, 7.0 kPa, 11.81 kPa, 15.0 kPa, 19.12 kPa, and 31.6 kPa. At these aforementioned operating conditions, the equilibrium CO_2 loading was found to be 0.486, 0.525, 0.511, 0.589, 0.569, and 0.575 (mol CO_2/mol amine), respectively. The correlation between the equilibrium CO_2 loading obtained from the experimental data and the literature for 30 wt% benchmark MEA is shown in Table 3.3. The percentage average absolute relative deviation (% AARD) of the experimental and literature data was found to be 3.17 %, which is good and highly acceptable. Therefore, the experimental setup has been validated and can now be used to estimate the equilibrium CO_2 loading of the novel aqueous amine blend of BAE+DMAE.

Table 3.3 Comparison between the equilibrium CO_2 loading obtained from the literature and actual experiments performed for 30 wt% MEA under specified conditions of temperature and CO_2 partial pressure[a].

S. No.	T (K)	P_{CO2} (kPa)	α_{exp} (mol CO_2/mol amine)	α_{lit} (mol CO_2/mol amine)	ARD (%)	Reference
1.	313.15	2.2	0.486	0.471	3.09	Shen and Li [71]
2.	313.15	7.0	0.525	0.510	2.85	Ji et al. [15]
3.	313.15	11.81	0.511	0.524	2.54	Aronu et al. [36]
4.	313.15	15.0	0.589	0.564	4.24	Gao et al. [73]
5.	313.15	19.12	0.569	0.585	2.81	Tong et al. [72]
6.	313.15	31.6	0.575	0.595	3.48	Lee et al. [70]
				AARD % =	3.17	

[a]Standard uncertainties of u are u(T) = 1 K, u(P_{CO2}) = 0.05 kPa, u(m_{BAE}) = 0.001, u(C) = 0.01 mol/L and u(α) = 0.02 mol CO_2/mol amine.

3.4.2 Equilibrium CO_2 loading of the novel aqueous amine blend

The bubble column reactor, Chittick apparatus, and volumetric titration method were helpful for estimating the equilibrium CO_2 loading of the novel aqueous amine blend of BAE+DMAE in a semi-batch mode. The temperature varied from 298.15 to 333.15 K, partial pressure of CO_2 ranged from 10.13 to 25.33 kPa, mole fraction of activator (BAE) varied from 0.05 to 0.20, and solution concentration ranged from 1 to 3 mol/L. The novel aqueous amine blend of BAE+DMAE has not shown any solid precipitation on CO_2 loading, so the adverse effects of solid precipitation did not affect the experimental results. Design expert software of trial version 8.0.6 was used to prepare the 30 experimental run sets, whereas 37 different runs were created manually under the aforementioned operating conditions. All such experiments were performed on the lab scale at one atmospheric pressure. The correlation between equilibrium CO_2 loading corresponding to various manual run sets is shown in Table 3.4. The % AARD of these runs was 3.41 %, which is highly acceptable in nature.

Table 3.4 Experimental equilibrium CO_2 loading (α_{exp}) and calculated equilibrium CO_2 loading (α_{cal}) for the novel aqueous amine blend of BAE+DMAE under the specified operating condition at atmospheric pressure[a].

Run	Operating Parameters				Initial pH	Final pH	α_{exp}	α_{cal}	ARD %
	T (K)	P_{CO_2} (kPa)	m_{BAE}	C (mol/L)	(CO_2-unloaded)	(CO_2-loaded)	(mol CO_2/mol amine)	(mol CO_2/mol amine)	
1.	313.15	20.27	0.05	1	12.10	8.87	0.7679	0.7136	7.06
2.	313.15	20.27	0.10	1	12.10	8.82	0.7966	0.7650	3.96
3.	313.15	20.27	0.15	1	12.10	8.80	0.8337	0.8212	1.49
4.	305.15	20.27	0.20	1	12.12	8.75	0.8932	0.9209	3.10
5.	313.15	20.27	0.20	1	12.18	8.86	0.8597	0.8822	2.62
6.	313.15	10.13	0.20	1	12.18	9.17	0.7306	0.7145	2.19
7.	313.15	15.20	0.20	1	12.08	8.99	0.7966	0.8113	1.85
8.	313.15	25.33	0.20	1	12.18	8.71	0.9365	0.9271	1.00
9.	323.15	20.27	0.20	1	12.12	8.99	0.8165	0.8321	1.91
10.	323.15	25.33	0.20	1	12.17	8.98	0.8628	0.8769	1.64
11.	333.15	20.27	0.20	1	12.14	9.25	0.7625	0.7800	2.30
12.	313.15	20.27	0.05	2	12.22	9.23	0.6561	0.5970	8.99
13.	313.15	20.27	0.10	2	12.01	9.24	0.6970	0.6484	6.96
14.	313.15	20.27	0.15	2	12.23	9.15	0.7380	0.7046	4.52
15.	298.15	20.27	0.20	1	12.16	8.77	0.9161	0.9537	4.11
16.	298.15	20.27	0.20	2	12.21	8.83	0.8165	0.8371	2.53
17.	305.15	20.27	0.20	2	12.23	8.94	0.7966	0.8043	0.97

18.	313.15	20.27	0.20	2	12.25	9.20	0.7658	0.7656	0.02
19.	313.15	10.13	0.20	2	12.24	9.50	0.6163	0.5979	2.97
20.	313.15	15.20	0.20	2	12.22	9.38	0.6693	0.6947	3.80
21.	313.15	25.33	0.20	2	12.21	9.01	0.7853	0.8105	3.20
22.	323.15	20.27	0.20	2	12.23	9.30	0.6892	0.7155	3.82
23.	323.15	25.33	0.20	2	12.20	9.27	0.7356	0.7603	3.37
24.	333.15	20.27	0.20	2	12.24	9.41	0.6649	0.6634	0.21
25.	313.15	20.27	0.05	3	12.22	9.57	0.5955	0.5501	7.61
26.	313.15	20.27	0.10	3	12.25	9.54	0.6352	0.6015	5.30
27.	313.15	20.27	0.15	3	12.30	9.52	0.6793	0.6577	3.17
28.	298.15	20.27	0.20	3	12.27	9.27	0.7501	0.7902	5.35
29.	305.15	20.27	0.20	3	12.28	9.18	0.7397	0.7574	2.39
30.	313.15	20.27	0.20	3	12.30	9.27	0.7091	0.7187	1.35
31.	313.15	10.13	0.20	3	12.27	9.64	0.5536	0.5510	0.45
32.	313.15	15.20	0.20	3	12.25	9.40	0.6070	0.6478	6.73
33.	313.15	25.33	0.10	3	12.26	9.27	0.6970	0.6463	7.26
34.	313.15	25.33	0.15	3	12.29	9.22	0.7169	0.7025	1.99
35.	313.15	25.33	0.20	3	12.26	9.28	0.7417	0.7635	2.95
36.	323.15	20.27	0.20	3	12.23	9.54	0.6439	0.6686	3.83
37.	333.15	20.27	0.20	3	12.18	9.64	0.5974	0.6165	3.20
								AARD % =	3.41

[a]Standard uncertainties u are u(T) = 1 K, u(P_{CO_2}) = 0.05 kPa, u(m_{BAE}) = 0.001, u(C) = 0.01 mol/L and u(α) = 0.02 mol CO_2/mol amine.

3.4.2.1 Temperature effect on equilibrium CO_2 loading for the BAE+DMAE novel aqueous amine blend

The effect of temperature on equilibrium CO_2 loading was analyzed by performing the CO_2 absorption experiments at temperatures ranging from 298.15 to 333.15 K by keeping constant P_{CO2} = 20.27 kPa and m_{BAE} = 0.20. Initially, the maximum value of equilibrium CO_2 loading was found at the lowest temperature, and the minimum value was achieved at the highest temperature at a particular value of solution concentration, which is shown in Figure 3.3 (a). Similar trends of temperature effect on equilibrium CO_2 loading were obtained for each solution concentration of 1 mol/L, 2 mol/L, and 3 mol/L. The prime reason for the lowest equilibrium CO_2 loading at the highest temperature is that the equilibrium shifts in the reverse direction as the temperature increases (i.e., Le Chatelier's principle) [1,8,20,26]. Another reason is that desorption of CO_2 gas molecules takes place on performing absorption at high temperature, leading to a reduction in the equilibrium CO_2 loading in the aqueous amine blend. Therefore, high temperature is not favorable for performing CO_2 solubility experiments either in the single aqueous amines or their various blends.

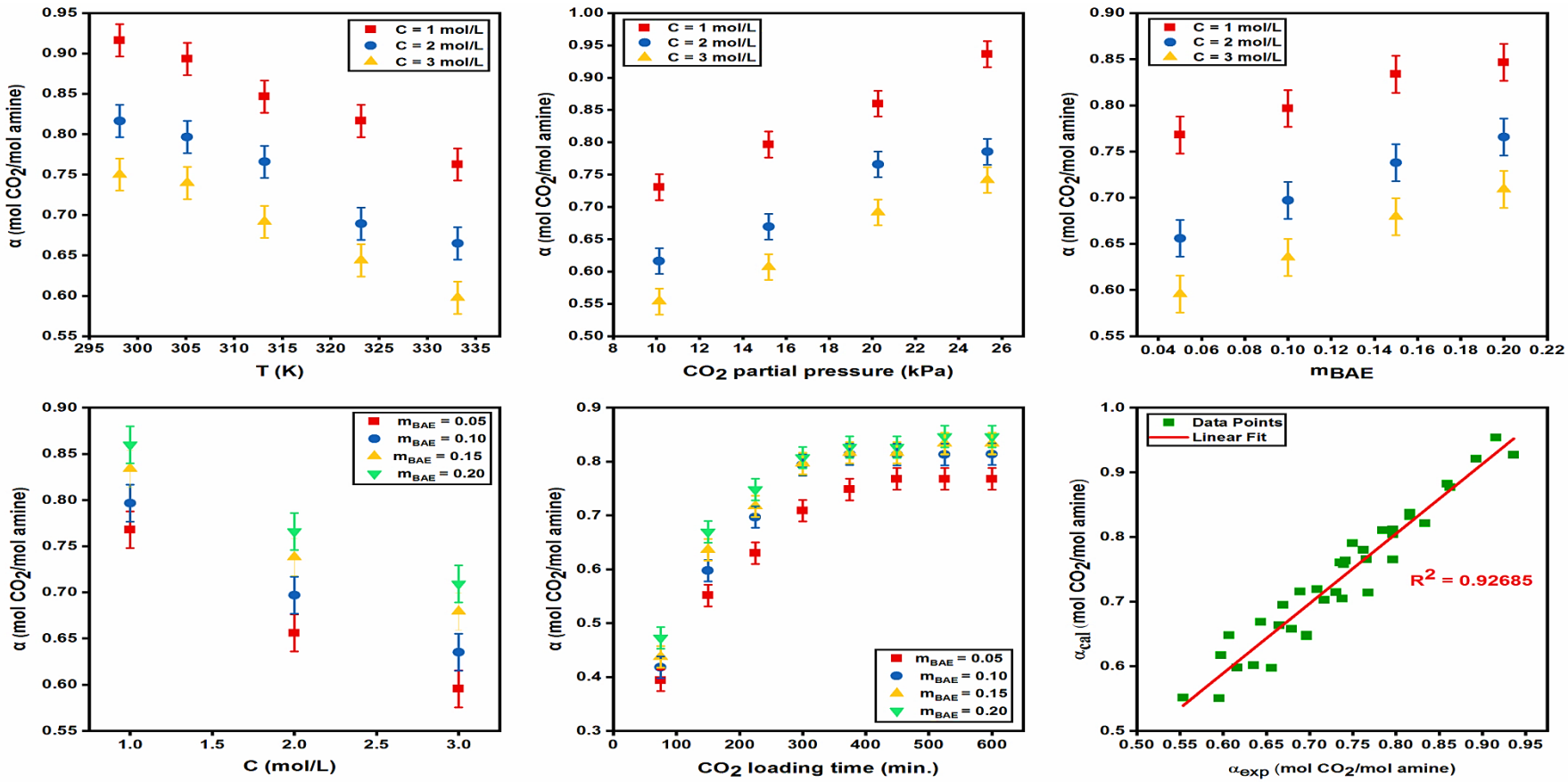

Figure 3.3 (a) Effect of temperature (T) on equilibrium CO_2 loading (α) for C = 1 mol/L, 2 mol/L, and 3 mol/L at constant P_{CO2} = 20.27 kPa and m_{BAE} = 0.20; (b) Effect of CO_2 partial pressure (P_{CO2}) on equilibrium CO_2 loading (α) for C = 1 mol/L, 2 mol/L, and 3 mol/L at constant T = 313.15 K and m_{BAE} = 0.20; (c) Effect of mole fraction of BAE (m_{BAE}) on equilibrium CO_2 loading (α) for C = 1 mol/L, 2 mol/L, and 3 mol/L at constant P_{CO2} = 20.27 kPa and T = 313.15 K; (d) Effect of solution concentration (C) on equilibrium CO_2 loading (α) for m_{BAE} = 0.05, m_{BAE} = 0.10, m_{BAE} = 0.15, and m_{BAE} = 0.20 at constant T = 313.15 K and P_{CO2} = 20.27 kPa; (e) Effect of CO_2 loading time on equilibrium CO_2 loading (α) for m_{BAE} = 0.05, 0.10, 0.15, and 0.20 at constant C = 1 mol/L, T = 313.15 K, and P_{CO2} = 20.27 kPa; (f) Parity plot of experimental (α_{exp}) and calculated (α_{cal}) CO_2 loading (α) for the novel aqueous amine blend of BAE+DMAE.

3.4.2.2 CO_2 partial pressure effect on equilibrium CO_2 loading for the BAE+DMAE novel aqueous amine blend

The effect of CO_2 partial pressure on equilibrium CO_2 loading was examined for three different amine blend solution concentrations, i.e., C = 1 mol/L, C = 2 mol/L, and C = 3 mol/L at constant T = 313.15 K and constant m_{BAE} = 0.20. CO_2 partial pressure ranging from 10.13 to 25.33 kPa was chosen to analyze the effect of CO_2 partial pressure on equilibrium CO_2 loading for the gas-liquid system. It was discovered that increasing the value of P_{CO2} the value α also increases accordingly, and this trend was followed for all different solution concentrations, which is shown in Figure 3.3 (b). According to Henry's law, the solubility of the gas in the liquid is directly proportional to the partial pressure of that particular gas. As a result, the experimental results show that the principle of Henry's law was correctly obeyed by this novel aqueous amine blend of BAE+DMAE. As the partial pressure of CO_2 increases, more CO_2 gas molecules dissolve in the liquid phase, obeying Henry's law and eventually forming a large amount of carbamate, carbonate, and bicarbonate. From Figure 3.3 (b), it is clearly evident that the equilibrium CO_2 loading continuously increased in the specified range of the CO_2 partial pressure. Similar trends of result correlating P_{CO2} vs. α and the effect of increasing P_{CO2} on α were also found in most of the literature [1,8,26].

3.4.2.3 Activator's mole fraction effect on equilibrium CO_2 loading for the BAE+DMAE novel aqueous amine blend

According to the majority of the literature, it was discovered that the primary and secondary amines could attain maximum equilibrium CO_2 loading up to 0.5 mol CO_2/mol amine, while tertiary amines can reach an equilibrium CO_2 loading of up to 1 mol CO_2/mol

amine [1,26]. Therefore, blending BAE (secondary amine) with DMAE (tertiary amine) was fruitful in order to attain maximum equilibrium CO_2 loading, increased reaction kinetics, enhanced absorption capacity, and less regeneration energy demand. In this chain, the effect of mole fraction of activator, i.e., BAE in the solution of BAE+DMAE at specific solution concentration, i.e., C = 1 mol/L, C = 2 mol/L, and C = 3 mol/L was examined in terms of equilibrium CO_2 loading. The partial pressure of CO_2 and temperature were kept constant at 20.27 kPa and 313.15 K, respectively. For each solution concentration, the value of m_{BAE} ranged from 0.05 to 0.20. As a result, the equilibrium CO_2 loading was calculated for each solution at m_{BAE} = 0.05, 0.10, 0.15, and 0.20. It is well evident from Figure 3.3 (c) that the value of equilibrium CO_2 loading increases on increasing the value of the mole fraction of BAE in the entire aqueous amine blend of BAE + DMAE. It was also found that the value of equilibrium CO_2 loading was maximum at m_{BAE} = 0.20 for every solution concentration of 1 mol/L, 2 mol/L, and 3 mol/L. Since BAE is a secondary amine, it has steric hindrance in its chemical structure, as well as a strong tendency to form bicarbonate and carbonate, resulting in a high equilibrium CO_2 loading. Therefore, increasing the value of the mole fraction of BAE in the aqueous amine blend of BAE+DMAE also increases the equilibrium CO_2 loading but, at the same time, also increases the heat of absorption. Taking into account the previous work of many researchers, they varied the mole fraction of the activator from 0.05 to 0.20 [1,20,22,25,26]. Therefore, for this present work, the value of the mole fraction of BAE was chosen from 0.05 to 0.20. This defined range of BAE increased the equilibrium CO_2 loading in the amine blend but did not drastically enhance the absorption heat.

3.4.2.4 Solution concentration effect on equilibrium CO_2 loading for the BAE+DMAE novel aqueous amine blend

The solution concentration has a significant role in capturing CO_2 for any aqueous amine blend. In this chain, the effect of solution concentration on equilibrium CO_2 loading for the novel aqueous amine blend of BAE+DMAE was analyzed for four different mole fraction of BAE ranging from 0.05 to 0.20 at constant T = 313.15 k and P_{CO2} = 20.27 kPa. Three different solutions of BAE+DMAE, i.e., C = 1 mol/L, C = 2 mol/L, and C = 3 mol/L, were prepared, and at various operating conditions, its effect on equilibrium CO_2 loading was examined. From Figure 3.3 (d), it was found that at least solution concentration, the value of equilibrium CO_2 loading was maximum and vice-versa. The trend of equilibrium CO_2 loading corresponding to solution concentration is as follows: 1 mol/L > 2 mol/L > 3 mol/L. This trend of decreasing equilibrium CO_2 loading with increasing solution concentration was observed for all m_{BAE} ranging from 0.05 to 0.20. Increasing the concentration of the solution inhibits the conversion of carbamate to bicarbonate, resulting in a lower equilibrium CO_2 loading [1,20,26]. Le Chatelier's principle states that as the composition of the amine blend enhances the number of reacting amine molecules increases, but simultaneously the ratio of amine to CO_2 increases, which results in a decrease in equilibrium CO_2 loading [1]. The overall experimental investigation concluded that the best equilibrium CO_2 loading was achieved to be 0.9365 mol CO_2/mol amine for C = 1 mol/L and m_{BAE} = 0.20 at constant T = 313.15 K and P_{CO2} = 25.33 kPa, as reported in Table 3.4 for a run number – 08. The whole description, as well as the effects of T, P_{CO2}, m_{BAE}, and C on equilibrium CO_2 loading, has already been discussed previously.

3.4.2.5 Absorption time effect on equilibrium CO_2 loading for the BAE+DMAE novel aqueous amine blend

Absorption time is a critical factor in determining how long any aqueous amine blend takes to achieve the condition of equilibrium CO_2 loading. Initially, the rate of CO_2 absorption is fast with respect to time, but it becomes sluggish when time proceeds, and at the maximum operating time, it becomes constant due to achieving the gas-liquid equilibrium. This is due to the fact that initially, the aqueous amine blend has the highest tendency to absorb CO_2, but as time proceeds, the solution's tendency to absorb CO_2 gets reduced. At maximum absorption time, no further absorption of CO_2 can take place because of achieving the situation of equilibrium CO_2 loading. For this current aqueous amine blend of BAE+DMAE, the absorption time effect was examined for the solution of concentration of 1 mol/L operated at constant T = 313.15 K and constant P_{CO2} = 20.27 kPa. An absorption time of 10 hours was chosen for the estimation of equilibrium CO_2 loading. The time effect was analyzed for four solutions with m_{BAE} ranging from 0.05 to 0.20. According to Figure 3.3 (e), the equilibrium CO_2 loading increased dramatically in the beginning, but after a while, the absorption decreased and became constant at the maximum CO_2 loading time.

3.4.3 Developing an empirical model for the novel aqueous amine blend of BAE+DMAE

It was so essential to validate the experimental results with an empirical model in order to prove the truthfulness of the experiments. An empirical model was developed by including temperature (T, in kelvin), partial pressure of CO_2 (P_{CO_2}, in kPa), mole fraction of BAE (m_{BAE}), and solution concentration (C, in mol/L), as independent variables. This developed model is valid at T = 298.15–333.15 K, P_{CO_2} = 10.13–25.33 kPa, m_{BAE} = 0.05–

0.20, and C = 1–3 mol/L. The model is useful for estimating the equilibrium CO_2 loading of the novel aqueous amine blend of BAE+DMAE. Based on the aforementioned parameters, the equation of the developed empirical model is as follows:

$$\alpha_{cal} = a_1 + a_2 T + a_3 T^2 + a_4 P_{CO2} + a_5 P_{CO2}^2 + a_6 m_{BAE} + a_7 m_{BAE}^2 + a_8 C + a_9 C^2 \quad (3.24)$$

Where α_{cal} is the equilibrium CO_2 loading (mol CO_2/mol amine) as calculated by the developed model equation, $a_1 - a_9$ are the unknown coefficients and other notations of Eq. (3.24) have already been discussed above.

The physical significance and reliability of this developed model have been found in most of the published literature [1,20,21,26]. The values of unknown coefficients involved in the above equation can be estimated with the help of using different experimental data sets. Microsoft Excel solver software benefitted in revealing these unknown values of the coefficients, and all these are listed in Table B3 of Appendix – B. By utilizing these unknown coefficients, the value of α_{cal} can be easily estimated for the specified set of operating conditions. The percentage absolute relative deviation (% ARD) and % AARD of α_{exp} and α_{cal} was determined by Eq. (3.25) and Eq. (3.26), respectively.

$$\% \text{ ARD} = \frac{|\alpha_{exp} - \alpha_{cal}|}{\alpha_{exp}} \times 100 \quad (3.25)$$

$$\% \text{ AARD} = \frac{1}{N} \times \sum_{i=1}^{N} \frac{|\alpha_{exp} - \alpha_{cal}|}{\alpha_{exp}} \times 100 \quad (3.26)$$

Where N denotes the total number of experiments, α_{exp} is the experimental equilibrium CO_2 loading (mol CO_2/mol amine), and α_{cal} represents the equilibrium CO_2 loading calculated by the developed model equation (mol CO_2/mol amine). The relationship between α_{exp} (by Eq. 3.1) and α_{cal} (by Eq. 3.24) has shown in Figure 3.3 (f). For the entire experimental run sets, the % AARD value was found to be 3.41 % which is a marvelous

agreement of experimental equilibrium CO_2 loading (α_{exp}) and the model's calculated equilibrium CO_2 loading (α_{cal}). Therefore, the developed model equation for calculating equilibrium CO_2 loading is highly accurate, reliable, and entirely acceptable.

3.4.4 Study of CO_2 desorption results

In the industrial context, cyclic capacity and cyclic equilibrium CO_2 loading are critical factors in choosing an appropriate solvent for the CO_2 capture process [1,8,39]. An amine's cyclic capacity is defined as its ability to capture CO_2 per mole of amine per amine cycle via a CO_2 capture unit. Cyclic capacity was found to be higher in amines with higher desorption rates [47]. The information on cyclic capacity plays a significant role in determining the value of regeneration efficiency of the CO_2 for any aqueous amine blend [22]. Desorption experiments were performed to determine the cyclic capacity and cyclic equilibrium CO_2 loading for the presently opted amine blend of BAE+DMAE. All these desorption experiments were conducted at a constant temperature and CO_2 partial pressure of 393.15 K and 25.33 kPa, respectively. The CO_2-saturated amine samples with solution concentration (C) of 1 mol/L, 2 mol/L, and 3 mol/L at T = 313.15 K, m_{BAE} = 0.20, and P_{CO2} = 25.33 kPa were chosen for conducting CO_2 desorption experiments. From Table 3.4, run no. 8, 21, and 35 were chosen for the entire investigation of cyclic capacity and cyclic equilibrium CO_2 loading. The data for conventional 30 wt% MEA was acquired from the study done by Pandey and Mondal [8], i.e., cyclic capacity = 0.22 mol CO_2/mol amine and cyclic equilibrium CO_2 loading ($\Delta\alpha$) = 1.082 mol CO_2/L solution. The desorption experiments were performed thrice, and the average value of CO_2 loading was finally chosen. After performing desorption experiments for 30 minutes, the CO_2 loading was found to be 0.2111, 0.1951, and 0.1240 mol CO_2/mol amine corresponding to solution

concentration of 1 mol/L (Run no. 8), 2 mol/L (run no. 21), and 3 mol/L (run no. 35), respectively. The cyclic capacity and cyclic equilibrium CO_2 loading of conventional 30 wt% MEA and the aqueous amine blend of BAE+DMAE at solution concentrations of 1 mol/L, 2 mol/L, and 3 mol/L are shown in Figure 3.4. The aqueous amine blend of BAE+DMAE at C = 3 mol/L demonstrated 71.23 % higher cyclic capacity than conventional 30 wt% MEA. This value claims that the size of the CO_2 capture unit would be smaller and require a low solvent circulation rate for the unique aqueous amine blend of BAE+DMAE.

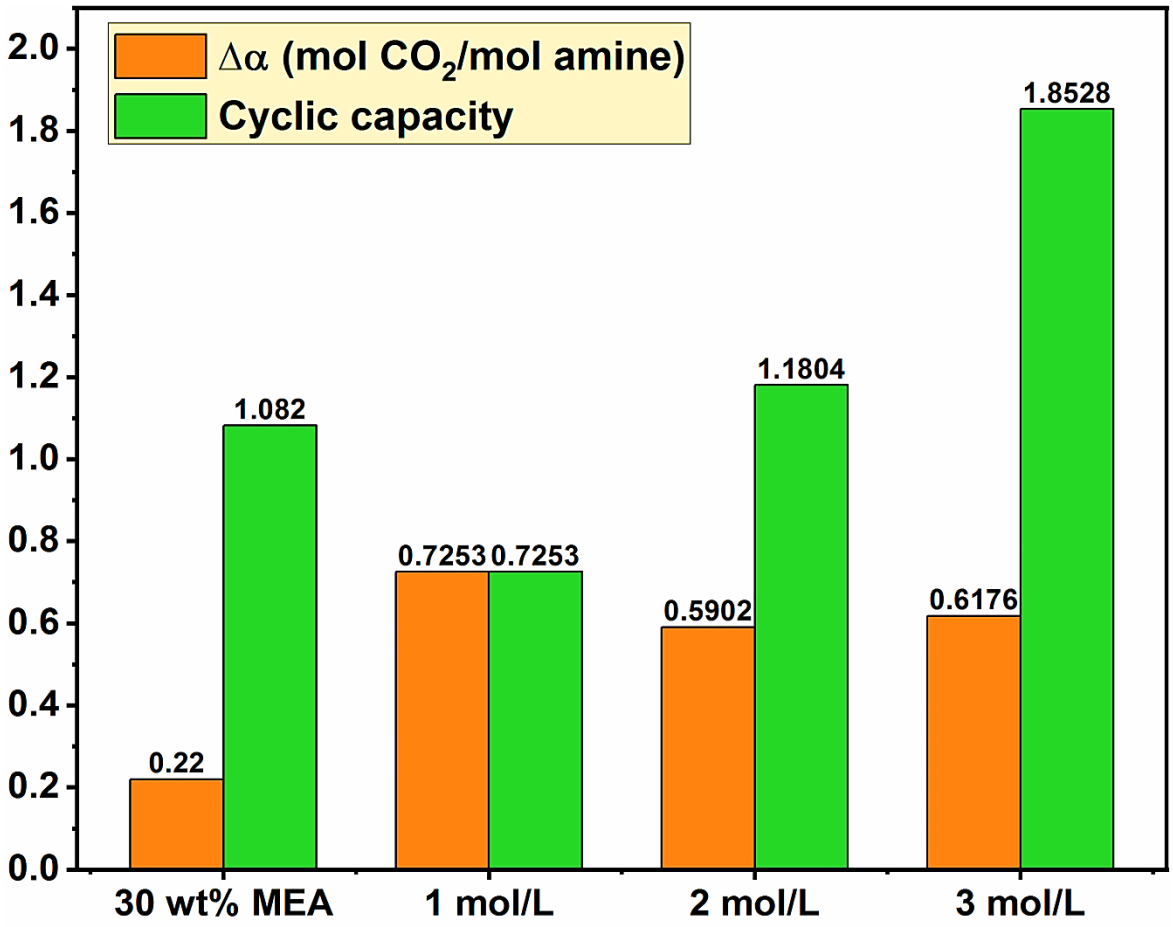

Figure 3.4 Cyclic equilibrium CO_2 loading and cyclic capacity of 30 wt% MEA (i.e., 5 mol/L) for the novel aqueous amine blend of BAE+DMAE with C = 1 mol/L, 2 mol/L, and 3 mol/L at constant m_{BAE} = 0.20.

3.4.5 Heat duty and regeneration efficiency investigation

Heat duty is the amount of external heat required while performing the desorption experiments in order to remove the CO_2 from the CO_2-saturated aqueous amine blend [13,34,39]. Narku-Tetteh et al. [47], in their investigation of heat duty, concluded that the heat duty requirement for regenerating the conventional 30 wt% MEA was 450 kJ/mol CO_2. The value of heat duty for benchmark MEA was acquired from their study to compare the results of this current aqueous amine blend of BAE+DMAE. Highly stable carbamate formation is the main reason for the maximum heat duty demand in the case of conventional MEA [13]. According to Eq. 3.7, in the correlation of heat duty, the value of the heat transfer rate becomes constant for the opted regeneration apparatus. Now, the heat duty is inversely proportional to the cyclic capacity. The value of cyclic capacity of the aqueous amine blend plays a significant role in determining the heat duty. Therefore, the experimental cyclic capacity of the aqueous amine blend follows the following trends with respect to solution concentration as: 3 mol/L > 2 mol/L > 1 mol/L. A similar trend for cyclic capacity corresponding to solution concentration was also found in our previous work [1]. The relationship between the heat duty and the solution concentration was compared with conventional MEA and is shown in Figure 3.5 (a).

The heat duty for 1 mol/L, 2 mol/L, and 3 mol/L was found to be 288.55 kJ/mol CO_2, 177.31 kJ/mol CO_2, and 112.96 kJ/mol CO_2, respectively. In comparison to conventional MEA, heat duty was reduced by 35.87 %, 60.59 %, and 74.89 % for 1 mol/L, 2 mol/L, and 3 mol/L, respectively. The effect of the BAE (activator) molar ratio in the aqueous solution of BAE+DMAE showed a significant impact on heat duty.

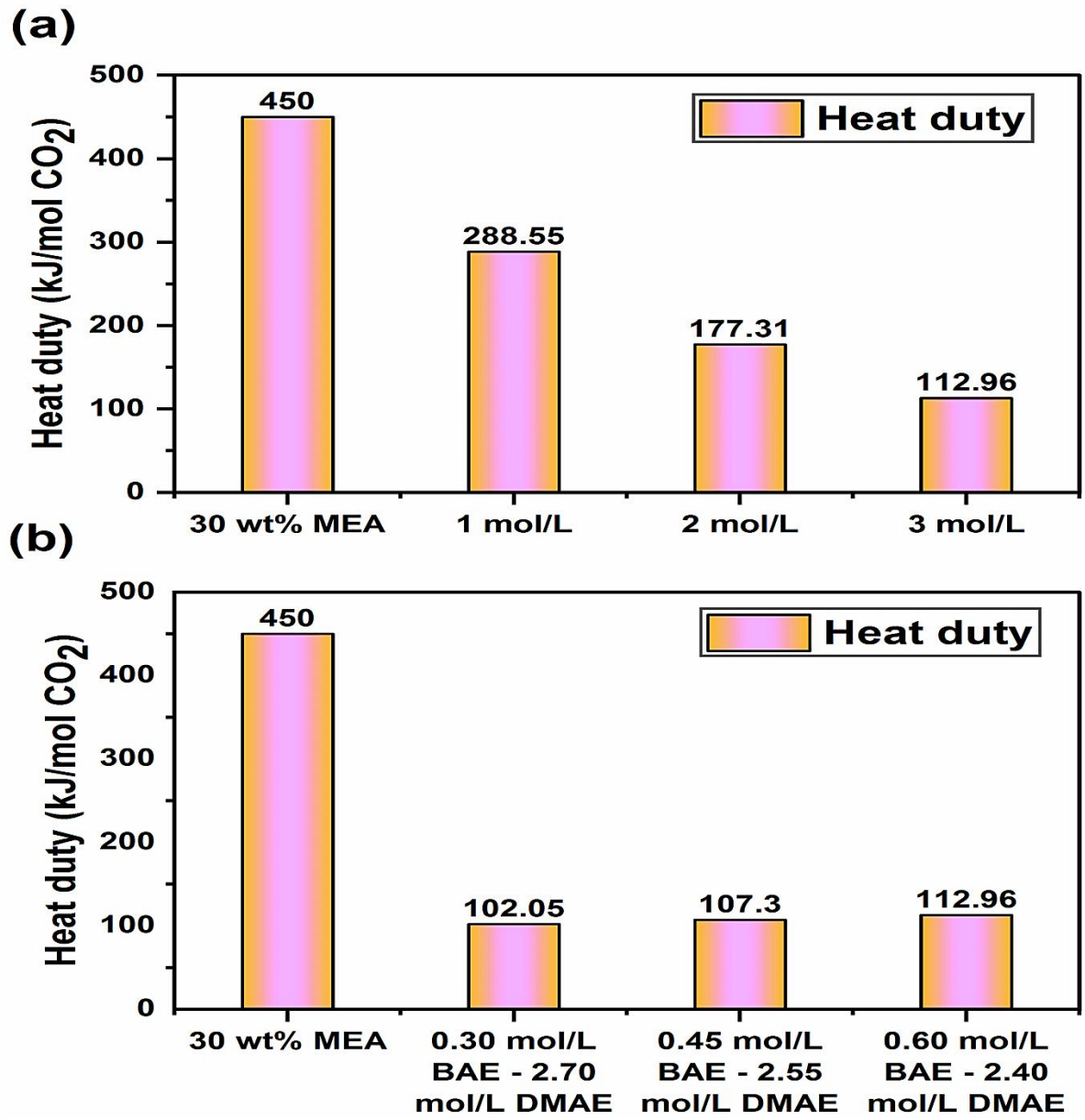

Figure 3.5 The relationship between the heat duty and the solution concentration; (a) Comparison in between the heat duty values for 30 wt% MEA and the novel aqueous amine blend of BAE+DMAE for C = 1 mol/L, 2 mol/L, and 3 mol/L; (b) Effect of increasing BAE molar ratio in the aqueous solution of BAE+DMAE on heat duty.

Wai et al. [34] and Muchan et al. [13] validated the above-mentioned results by correlating the effect of the activator's molar ratio and heat duty of regeneration at constant solution composition. The value of heat of absorption and HCO_3^- ion formation enhances by increasing the molar ratio of the activator in the entire solution composition, consequently increasing the heat duty requirement during regeneration. The trend of heat duty on increasing the molar ratio of BAE in the current aqueous amine blend of BAE+DMAE is as follows: 30 wt% MEA > 0.60 mol/L BAE – 2.40 mol/L DMAE > 0.45 mol/L BAE – 2.55 mol/L DMAE > 0.30 mol/L BAE – 2.70 mol/L DMAE. The relationship between the heat duty and the effect of the molar ratio of BAE in the amine blend is shown in Figure 3.5 (b). The regeneration efficiency of the aqueous amine of BAE+DMAE with solution concentrations of 1 mol/L, 2 mol/L, and 3 mol/L was found to be 77.45 %, 75.15 %, and 83.27 %, respectively. The regeneration efficiency is high and showed almost similar results for all of the aforementioned solution compositions.

3.4.6 Investigation on heat of CO_2 absorption (ΔH_{abs})

The calorimeter is the instrument that can experimentally determine the value of ΔH_{abs} whereas theoretically, it can be calculated by using the Gibbs-Helmholtz equation, as already discussed in section 3.2.7. For the present aqueous amine blend of BAE+DMAE (C = 1 mol/L), the Gibbs-Helmholtz equation has been opted because it produces reliable results that are comparable to the calorimetric results as reported in the majority of the studies [1,63-65]. At different operating conditions, there were few data points at which the value of equilibrium CO_2 loading was almost similar. For this present experimental work on the BAE+DMAE amine blend, three different data points of T and P_{CO2} at nearly similar equilibrium CO_2 loading of 0.86 and 0.90 mol CO_2/mol amine, respectively, were chosen to

estimate the heat of CO_2 absorption. A graph between d $[(\frac{1}{T})]$ and d $[\ln(P_{CO2})]$ was plotted at constant α = 0.86 and α = 0.90 mol CO_2/mol amine, which is shown in Figure 3.6.

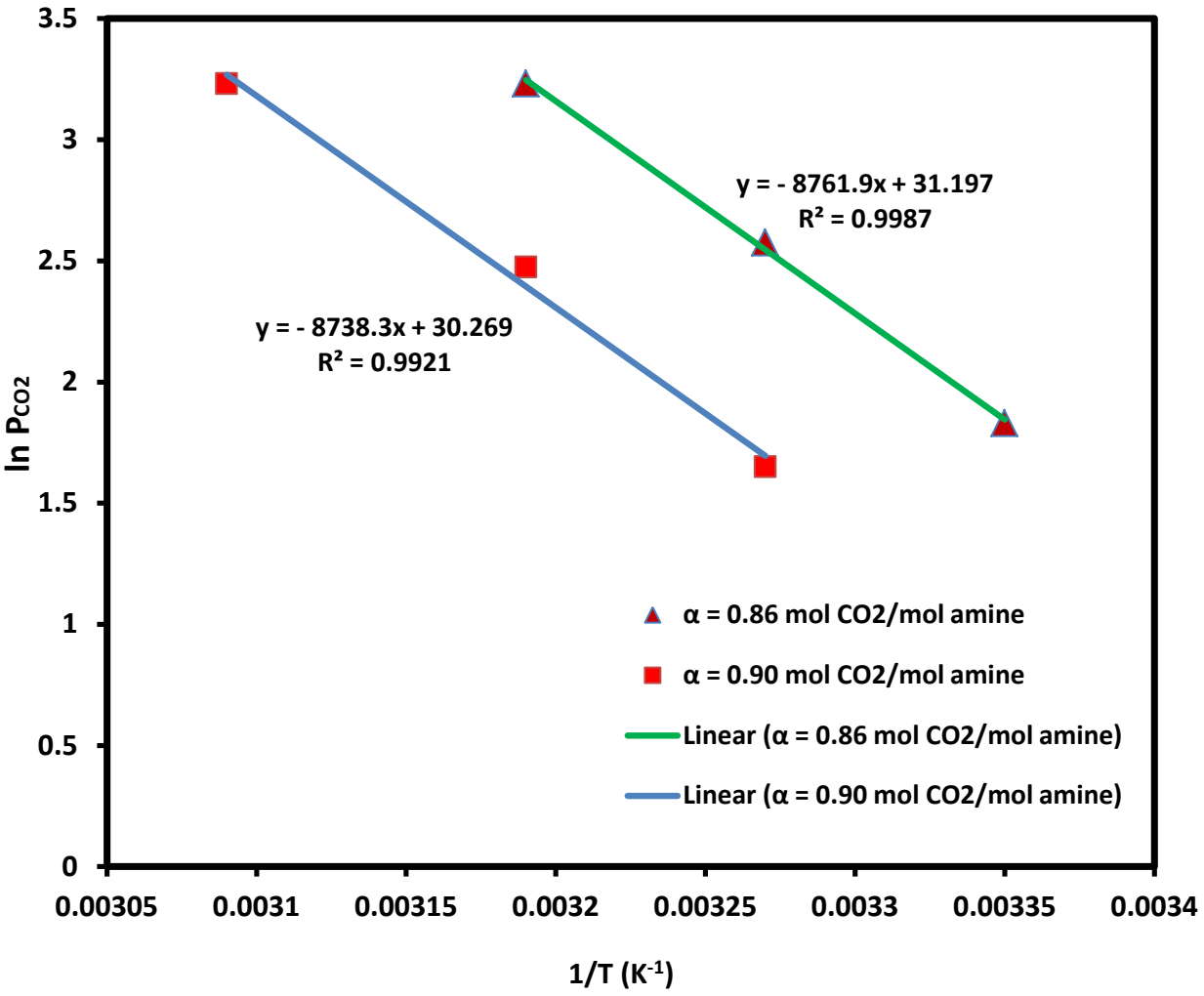

Figure 3.6 Plot of $\ln(P_{CO2})$ vs. (1/T) at different values of equilibrium CO_2 loading (i.e., α = 0.86 and 0.90 mol CO_2/mol amine) for the determination of ΔH_{abs} for the novel aqueous amine blend of BAE+DMAE.

The method of estimating the value of ΔH_{abs} has already been described in the previous section of 3.2.7. The slope of the line at $\alpha = 0.86$ and $\alpha = 0.90$ was found to be -8761.9 and -8738.3, respectively. The value of heat of CO_2 absorption corresponding to the above-mentioned values of the slope was achieved to be -72.84 kJ/mol and -72.65 kJ/mol, respectively. The average value of ΔH_{abs} for the aqueous amine blend of BAE+DMAE at C = 1 mol/L and $m_{BAE} = 0.20$ was found to be -72.74 kJ/mol. The negative symbol in the value of ΔH_{abs} signifies that the amine blend in reaction with CO_2 is exothermic in nature. The value of ΔH_{abs} (-72.74 kJ/mol) for the chosen amine blend system is higher than traditional tertiary amine (MDEA = -54.6 kJ/mol) but lower than conventional primary amines (MEA = -85.13 kJ/mol) [33,45].

3.4.7 Effect of pH on various amine blend samples

It is well known that amines are basic in nature, and CO_2 gas is acidic. The significant effects of the change in pH of the amine blend solution can be seen after successful CO_2 loading in the aqueous amine blend of BAE+DMAE. As discussed previously, the intermediate complexes of bicarbonate and carbonate were also formed on CO_2 loading. The pH of all the CO_2-unloaded and CO_2-loaded samples for the current amine blend was experimentally found to be in the range of 12.01–12.30 and 8.71–9.64, respectively, as reported in Table 3.4. As the CO_2 loading in the amine blend increases over time, the pH of the solution decreases [12]. A similar pH trend was observed for the chosen amine blend, and the pH decrement was faster initially up to a certain time range, but after that, a slight change in pH was observed [48]. At C = 1 mol/L, 2 mol/L, and 3 mol/L, all 37 runs with the different values of pH before and after CO_2 loading have been reported in Table 3.4. For run-08 (T = 313.15 K, P_{CO2}= 25.33 kPa, $m_{BAE} = 0.20$, and C = 1 mol/L), the maximum

equilibrium CO_2 loading of 0.9365 mol CO_2/mol amine was achieved, consequently resulting in the lowest pH of 8.71. The absorbed CO_2 in the aqueous amine blend of BAE+DMAE gets liberated during the desorption experiments, and the pH of the CO_2-regenerated solution returns back approximately to its initial value. Samples of amine blend from run no. - 08, 21, and 35 were chosen and were regenerated for their pH assessment. T, P_{CO2}, and m_{BAE} of these particular amine blends were kept constant, and only solution concentration variation was considered. Finally, regenerated pH values of 10.51, 10.38, and 10.88 were obtained for run no. 08, 21, and 35, respectively. The pH of CO_2-regenerated amine blend samples is slightly lower than that of CO_2-unloaded samples because the least amount of CO_2 is still left even after performing complete regeneration. It can be concluded from these values that the pH of the regenerated amine blend samples lies in the range of 10–11, and the change in solution concentration has a negligible effect on the pH value.

3.4.8 FTIR investigations

Before performing the actual experiments, the novel CO_2-unloaded aqueous amine solution was prepared on the lab scale comprising BAE and DMAE. Because of the presence of BAE as a secondary amine in the aqueous solution, the characteristic peaks at 3440.95, 3423.95, and 3442.66 cm^{-1} were obtained, corresponding to CO_2-unloaded, CO_2-loaded, and CO_2-regenerated amine samples, respectively, as shown in Figure 3.7. These characteristic peaks demonstrate either asymmetric or symmetric N–H stretching behavior of BAE. A similar trend of peaks corresponding to BAE was also found in the study performed by Ping et al. [31] and Im et al. [74].

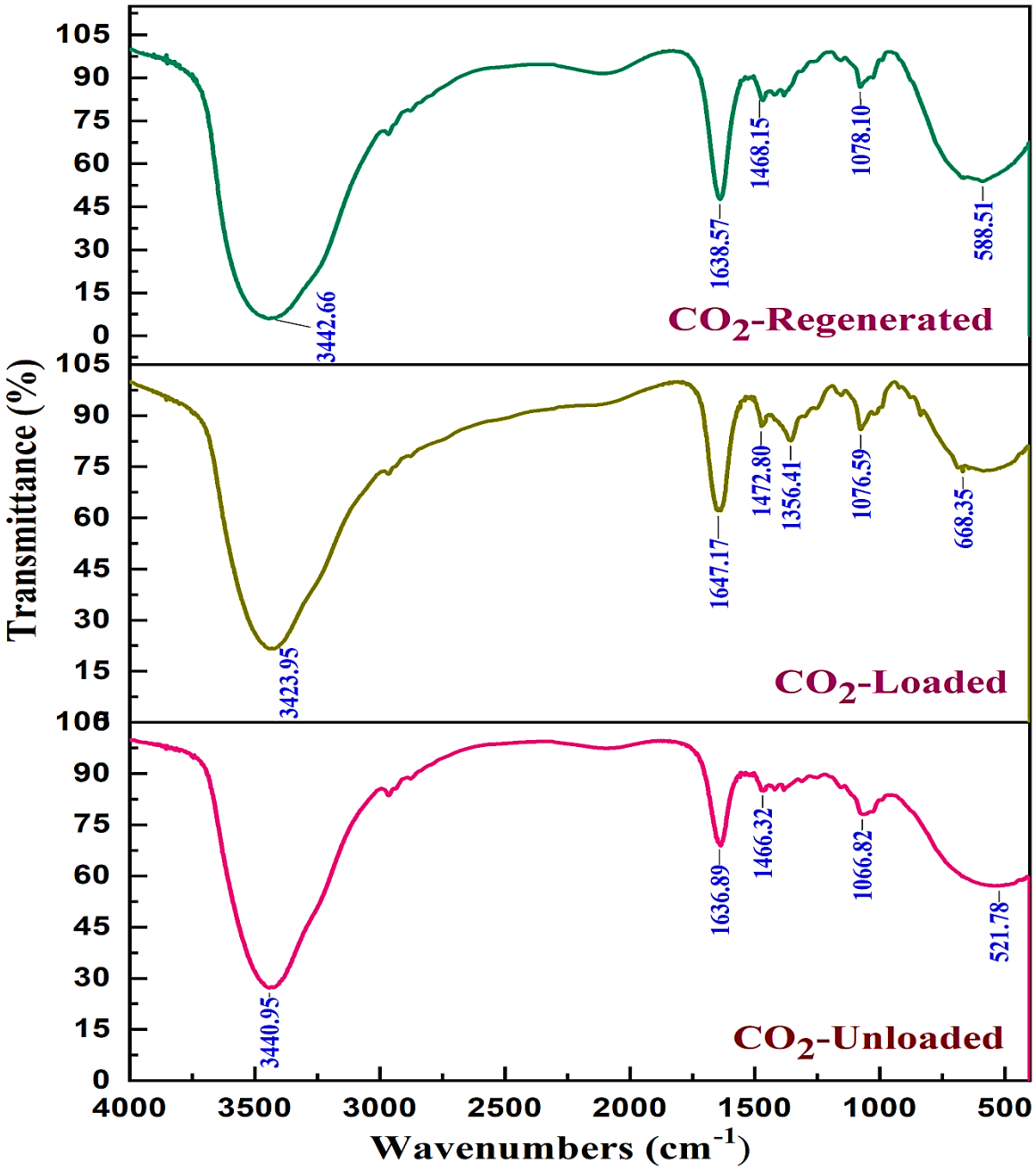

Figure 3.7 FTIR analyses of species present in CO_2-unloaded sample, CO_2-loaded sample, and CO_2-regenerated sample for the aqueous amine blend of BAE+DMAE.

One characteristic peak was obtained for the CO_2-loaded amine blend sample at 1356.41 cm^{-1}, indicating the formation of the carbamate (i.e., carbonate or bicarbonate products). This peak has been acquired due to the asymmetric carbonyl stretching ($-COO^-$) and asymmetric C–N stretching of $-NCOO^-$ behavior of the sample [29,31]. The aforementioned carbamate peak was absent in the CO_2-unloaded and CO_2-regenerated amine blends, as shown in Figure 3.7. The dearth of CO_2 in the CO_2-unloaded and CO_2-regenerated amine blend samples is mainly responsible for it, as authenticated by the FTIR test. NH_2^+ deformation is due to the protonation of amine, and due to $C=O$ stretching, the characteristic peaks were obtained at 1636.89, 1647.17, and 1638.57 cm^{-1}, corresponding to CO_2-unloaded, CO_2-loaded, and CO_2-regenerated amine blends, respectively [16,29,75,76]. In all three amine samples, the characteristic peaks at 1466.32, 1472.80, and 1468.15 cm^{-1} were due to the stretching vibration of the C–O bond [76]. For the present opted novel amine blend, the peaks at 521.78, 668.35, and 588.31 cm^{-1} occurred due to the presence of DMAE (i.e., tertiary amine), which was also validated by Ohno et al. [77] in their study. C-N stretching vibration peaks of CO_2-unloaded, CO_2-loaded, and CO_2-regenerated amine samples were obtained at 1066.82, 1076.59, and 1078.10 cm^{-1}, respectively [75].

3.4.9 ^{13}C NMR investigation of species in the novel aqueous amine blend

^{13}C NMR spectroscopic analysis was done to reveal the presence of species on CO_2-unloaded, CO_2-loaded, and CO_2-regenerated aqueous amine blend of BAE+DMAE. Any of the amine blend samples can be chosen for the NMR investigation, so for this present study, the run–08 sample was selected for the NMR investigation because of its highest equilibrium CO_2 loading (α_{exp} = 0.9365 mol CO_2/mol amine). The NMR result of the CO_2-unloaded amine blend sample is shown in Figure 3.8 (a), and several peaks were identified

in the frequency range of 13.84 and 60.18 ppm. The signals at 13.84, 20.02, and 31.03 ppm are owing to the presence of BAE in the BAE+DMAE amine blend. Similar trends of results for the BAE peaks were also found in some literature [37,44]. Similarly, peaks available at 44.72, 44.75, 58.35, 58.92, 60.06, and 60.18 ppm represent the presence of DMAE in the amine blend. The abundance of DMAE peaks lying in the range of 44.72–60.18 ppm is also authenticated by the study conducted by several researchers [1,16,78]. Likewise, DMSO-d_6 was employed for signal locking; therefore, its peaks were revealed in the frequency range of 38–39 ppm.

After CO_2 gets absorbed in the amine blend of BAE+DMAE, then there is a formation of bicarbonate and carbonate species due to the chemical reaction, as previously discussed in section 3.3.1. The NMR analyses of the CO_2-loaded amine blend sample are shown in Figure 3.8 (b). The arrival of a peak at 159.78 ppm occurred in the carbonyl region (C=O) because of the formation of bicarbonate/carbonate products after the CO_2 absorption. Most published research studies discovered that peaks in the range of 159–168 ppm are mainly responsible for the bicarbonate/carbonate species [1,14,16,18,37,44,46,78]. The chemical shifts of $BAEH^+$ and $DMAEH^+$ species were detected in the range of 13.47–27.87 ppm and 43.49–61.20 ppm region, respectively.

The CO_2-desorption experiments were conducted to estimate the cyclic equilibrium CO_2 loading, cyclic capacity, heat duty, and regeneration efficiency of the novel aqueous amine blend of BAE+DMAE. In such experiments, regeneration heat was supplied to the CO_2-loaded amine blends. This regeneration heat breaks the molecules of carbonate/bicarbonate and removes the CO_2 gas that had been initially absorbed in the aqueous amine blend. Figure 3.8 (c) authenticated the fact, as mentioned earlier, that the peak of

bicarbonate/carbonate that appeared in the CO_2-loaded sample vanished from the CO_2-regenerated sample in the NMR investigation. The abundance of BAE and DMAE peaks occurred in the range of 13.58–30.59 ppm and 44.46–59.86 ppm, respectively. These peaks of BAE and DMAE were just similar to the peaks for the CO_2-unloaded sample while performing the NMR investigation. In the CO_2-regenerated amine blend, a minor peak at a frequency of 70.88 ppm was also obtained, which could be attributable to the presence of a negligible quantity of contaminant in the sample. The presence of all the species in the CO_2-unloaded, CO_2-loaded, and CO_2-regenerated aqueous amine blend of BAE+DMAE has been listed in Table 5.

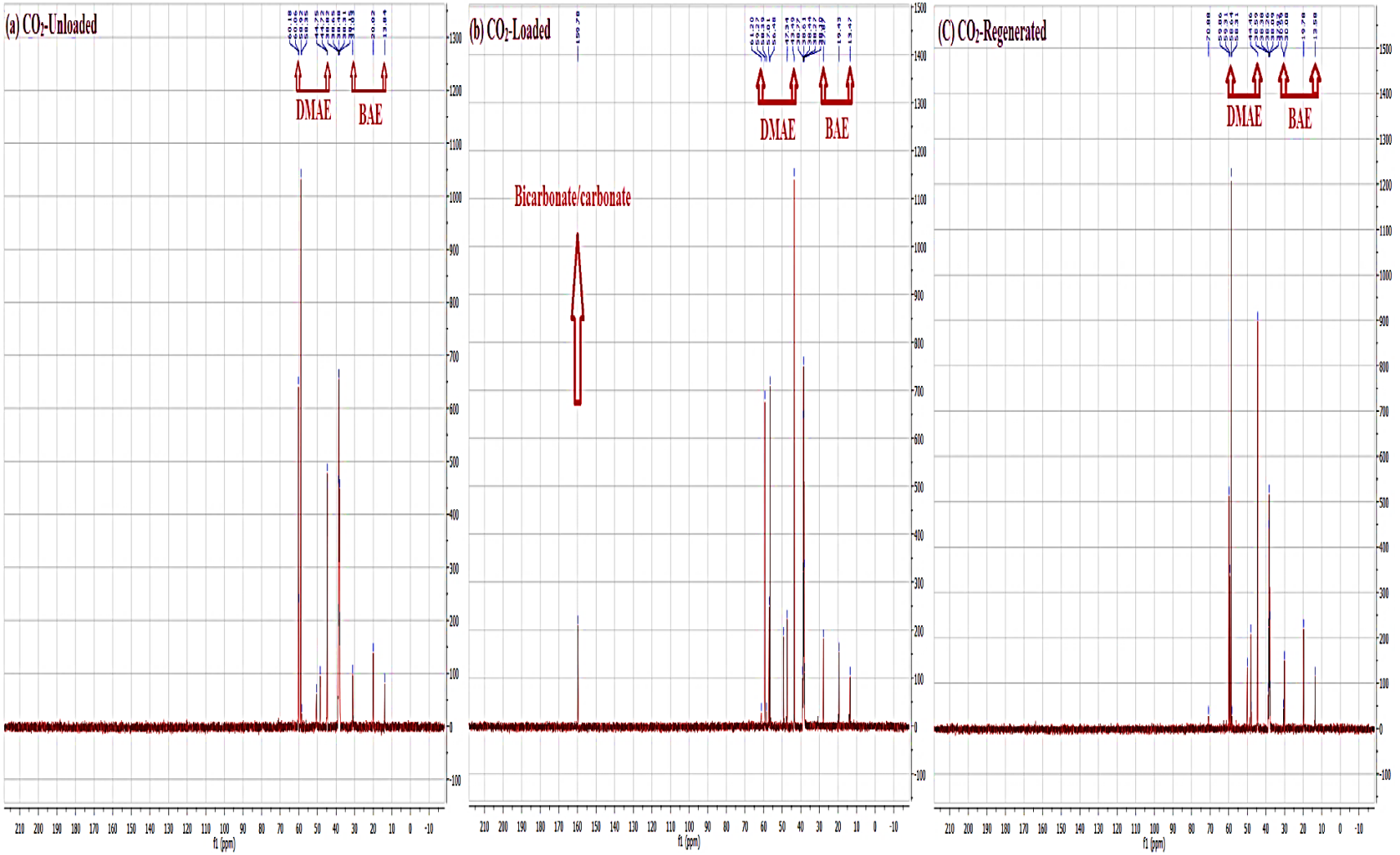

Figure 3.8 ^{13}C NMR investigation of species present in aqueous amine blend of BAE+DMAE; (a) CO_2-unloaded sample; (b) CO_2-loaded sample; (c) CO_2-regenerated sample.

Table 3.5 Identification of chemical species present in the CO_2-unloaded, CO_2-loaded and CO_2-regenerated aqueous amine blend of BAE+DMAE.

Compounds	Structure and identification	Spectral peak range (in ppm)
BAE	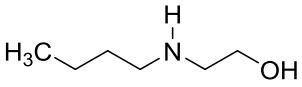	CO_2-unloaded: 13.84 – 31.03 CO_2-regenerated: 13.58 – 30.59
$BAEH^+$	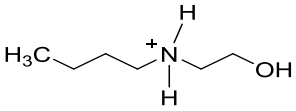	CO_2-loaded: 13.47 – 27.87
DMAE	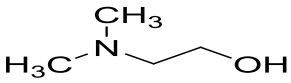	CO_2-unloaded: 44.72 – 60.18 CO_2-regenerated: 44.46 – 59.86
$DMAEH^+$	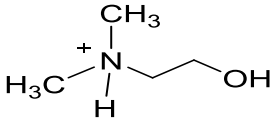	CO_2-loaded: 43.49 – 61.20
HCO_3^-	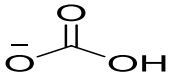	CO_2-loaded: 159.78
CO_3^{2-}	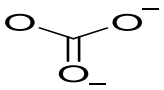	CO_2-loaded: 159.78

3.4.10 Study of toxicity level of BAE and DMAE

Amines and their degradable products mix with soil, water, and air due to spillage and exhaust gas from the CO_2 capture plants. Sometimes it is seen that during the transportation of various amines, leakage in the transportation vessel due to technical faults may cause severe environmental and human health issues. Assessment of toxicity of various chemicals can be done by considering the parameter of lethal dose (LD_{50}; mg/Kg). The higher value of LD_{50} represents the lower toxicity level of the amine and vice-versa. Based on conventional promising alkanolamine, MDEA, AMP, DMAE, PZ, DEA, Diethylethanolamine (DEEA), MEA, BAE, and 3-Dimethylamino-1-propanol (3DMAP) were considered for the toxicity assessment. Figure 3.9 shows the different values of LD_{50} for various amines. MDEA, AMP, DMAE, PZ, DEA, DEEA, MEA, and BAE are slightly toxic in nature (category 3^{rd}) with LD_{50} values of 4680, 2900, 2000, 1900, 1600, 1300, 1089, and 890 mg/Kg, respectively [79-86]. Only a single amine, 3DMAP, showed moderate toxicity behavior with an LD_{50} value of 442 mg/Kg (category 2^{nd}). Both the amines DMAE and BAE are slightly toxic, and they are used in this current work of CO_2 capture using a novel aqueous amine blend of BAE+DMAE. As a result, both amines, BAE and DMAE, can be recommended for CO_2 capture due to the least hazardous impact on environmental and human health aspects.

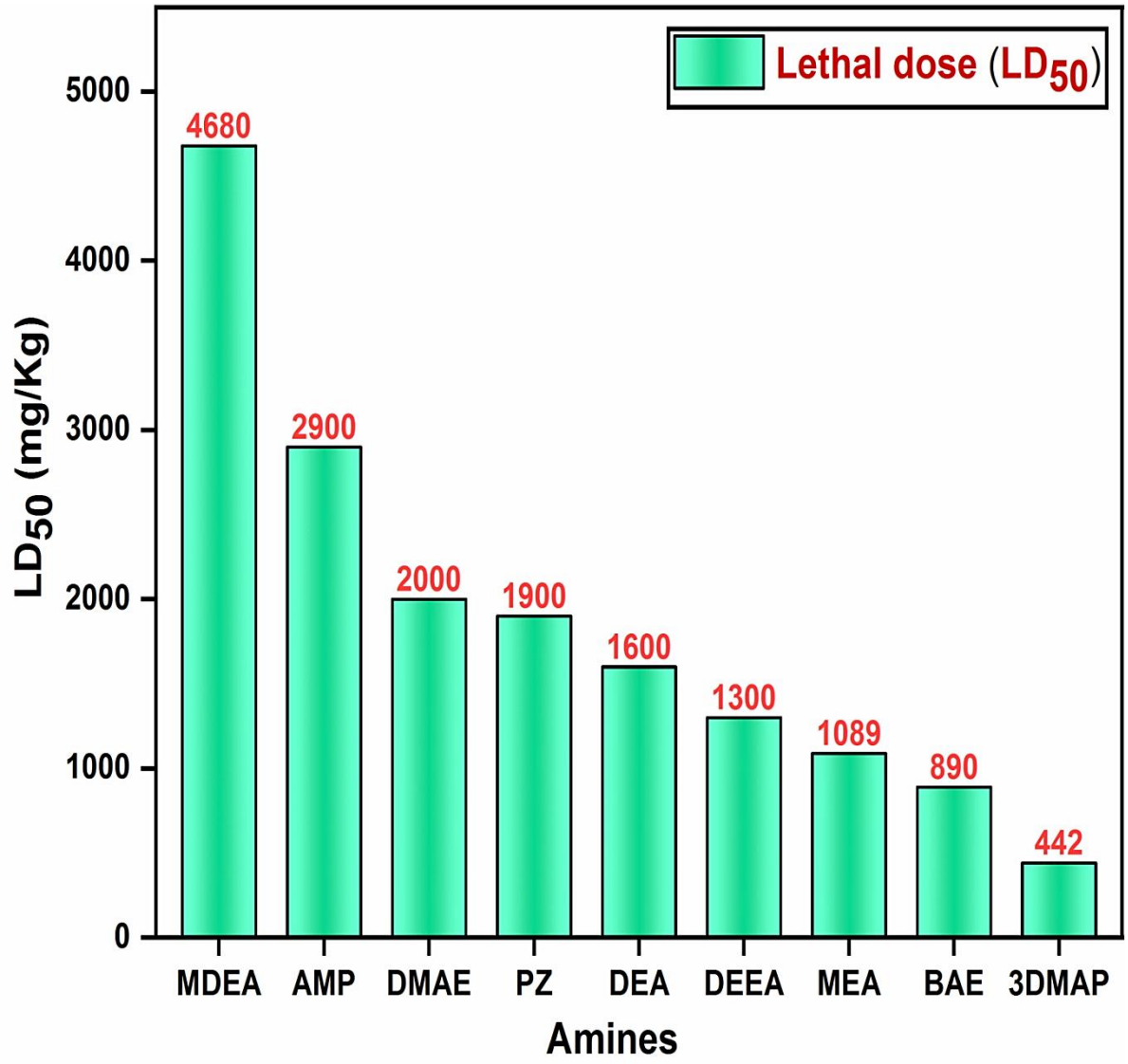

Figure 3.9 Value of toxicity represented in terms of lethal dose (LD_{50}) for various conventional amines.

3.4.11 Optimization by using response surface methodology (RSM) – a statistical approach

RSM is a statistical and mathematical approach for designing and developing experimental run sets for optimizing nearly all types of engineering problems [50,52-55,87]. RSM optimization of any engineering problem has grown in popularity in recent years, and it is now used by many researchers. It is a software-based approach that optimizes the entire independent variables (i.e., factors) and also correlates with the dependent variable as a final response. Before employing the RSM, it is essential to select an experimental design to obtain the final response [88]. The relationship between the experimental independent and dependent variables can be represented as:

$$Y = f(X_1, X_2, X_3, ..., X_N) + \mu \quad (3.27)$$

Where Y is the final response (i.e., dependent variables), X_1, X_2, X_3... X_N are the various independent variables involved in the experimental work, and μ is the error function for the chosen system. The RSM objective function's dependency is based on a regression model, and the objective function can be defined in either first or second order [1,62]. The regression model so obtained from RSM establishes a correlation between the final response and the independent variables. This mathematical tool selects the appropriate model, develops the model equation, and at last evaluates the value of all the unknown coefficients present in the model equation [1]. An empirical model is developed in terms of a polynomial equation and these equations can be linear, two-factor interaction (2 FI), quadratic, and cubic in nature [52,57]. A generalized quadratic model can be defined as:

$$Y = \tau_0 + \sum_{i=1}^{n} \tau_i x_i + \sum_{i=1}^{n} \tau_{ii} x_i^2 + \sum_{i=1}^{n} \sum_{j>1}^{n} \tau_{ij} x_i x_j + \mu \quad (3.28)$$

Where Y denotes the ultimate response, τ_0 denotes the constant coefficient, τ_i is the linear constant coefficient, τ_{ii} represents the squared interaction or quadratic constant coefficients, τ_{ij} represents the mutual interaction coefficients, and μ is the random error. ANOVA and lack-of-fit tests were targeted to judge the model's fitness [51]. If a significant result for regression and a non-significant result for the lack-of-fit tests are obtained, the developed model is assumed to be fit for the entire experimental run [1,88]. R-square and adjusted R-square values are used to assess the fitness of the developed model for first or second-order models. When the R-square value is greater than 0.5, and the adjusted R-square value is close to 1, the first-order model is acceptable [1,62].

Design-Expert® software of trial version 8.0.6 developed by Stat-Ease was used for the optimization and the CCD approach was adopted amongst various available designing tools. For this present experimental work, four operating parameters, i.e., Temperature (T), CO_2 partial pressure (P_{CO2}), mole fraction of activator (m_{BAE}), and solution concentration (C) were optimized, and corresponding to these parameters, optimum final response (Y) in terms of equilibrium CO_2 loading has been calculated. T = 298.15–333.15 K, P_{CO2} = 10.13–25.33 kPa, m_{BAE} = 0.05–0.20, and C = 1–3 mol/L were the initially assigned range of all the independent variables. A 2^4 full factorial CCD was adopted to prepare the entire run sets, and these runs have 16 factorial points, 8 axial points, and 6 repeating central points. This can be represented in a generalized form as:

$$N = 2^n + 2n + n_{centre} = 2^4 + 2.4 + 6 = 30 \quad (3.29)$$

Where N is the total number of experimental runs generated by the software, n is the number of independent variables and n_{centre} is the number of central points involved in the whole system.

All such 30 experimental runs at various operating condition of T, P_{CO2}, m_{BAE}, and C were generated by the RSM software. All experiments were conducted in the same order as provided by the software. By actually performing the experiments, the value of equilibrium CO_2 as a final response corresponding to all of these generated experimental runs was input in the software. The RSM software then created an empirical model consisting of quadratic equations based on the experimental results [52]. The main advantage of using the RSM approach for optimization is to obtain the optimum values of independent variables and final response by creating the least number of experimental run sets. The main disadvantage of RSM optimization is that it cannot assess product quality.

3.4.11.1 RSM approach for establishing the correlation between factors and the final response

The primary goal of this work was to optimize the equilibrium CO_2 loading by using the RSM optimization technique for the novel aqueous amine blend of BAE+DMAE. In this work, T, P_{CO2}, m_{BAE} and C were the four factors on which the final response of the system depends. Initially, A, B, C, and D were assigned to the software corresponding to the factors T, P_{CO2}, m_{BAE} and C, respectively. Temperature (A) varied from 298.15–333.15 K, CO_2 partial pressure (B) ranged from 10.13–25.33 kPa, mole fraction of BAE (C) changed from 0.05–0.20, and solution concentration (D) varied from 1–3 mol/L. Based on various designing approaches, CCD opted and the quadratic model was chosen to optimize the value of equilibrium CO_2 loading. RSM generated a total of 30 experimental runs consisting of 24 non-central and 6 central points, and these runs were based on the range of factors that were input to the software. Table 3.6 indicates all the independent variables as factors and their coded levels, which are found in the design summary part of the RSM

software. Every experiment was performed in the same manner as provided by the software. Figure A6 (a), (b), (c), and (d) of the Appendix – A represents the relationship between the number of experiments and the equilibrium CO_2 loading as a final response lying at a particular range of temperature, CO_2 partial pressure, mole fraction of BAE, and solution concentration, respectively. The experiments were performed on the lab scale, and the values of equilibrium CO_2 loading (Y) were finally estimated under specific operating conditions. The final response, 'Y', corresponding to each experimental run set was inputted into the software for further analyses.

Table 3.7 shows the various experimental run sets generated by the RSM software under various operating conditions. Run numbers 1–16 show the factorial points; 17–24 show the axial points; and 25–30 show the center points. The value of Cook's distance of all the 30 experimental runs suggested that its value lies in the range of 0 to 1.

Table 3.6 Coded levels of all the independent variables used in the experiment of evaluating the equilibrium CO_2 loading as a final response (Y) by using central composite design in the RSM software.

Factors	**Unit**	**Symbol**	**Coded Levels**				
			- α	**- 1**	**0**	**+ 1**	**+ α**
Temperature	K	A	298.15	306.90	315.65	324.40	333.15
Partial pressure of CO_2	kPa	B	10.13	13.93	17.73	21.53	25.33
Mole fraction of BAE	-	C	0.05	0.09	0.13	0.16	0.20
Solution concentration	mol/L	D	1	1.5	2	2.5	3

Table 3.7 Values of experimental equilibrium CO_2 loading as a final response (Y) and its predicted value for the runs created by the RSM software for the novel aqueous amine blend of BAE+DMAE under the specified operating condition at atmospheric pressure[a].

Run	Operating parameters				Point type	Cook's distance	Final response (Y)	α_{cal}	$\alpha_{Predicted}$	ARD* %
	T (K)	P_{CO_2} (kPa)	m_{BAE}	C (mol/L)			(mol CO_2/mol amine)	(mol CO_2/mol amine)	(mol CO_2/mol amine)	
1.	315.65	17.73	0.13	3	Factorial	0.085	0.5727	0.5787	0.58	1.05
2.	324.40	13.93	0.09	1.5	Factorial	0.000	0.6004	0.5914	0.60	1.49
3.	306.90	13.93	0.16	1.5	Factorial	0.022	0.7713	0.7893	0.79	2.34
4.	324.40	21.53	0.16	2.5	Factorial	0.056	0.6213	0.6059	0.60	2.46
5.	315.65	17.73	0.20	2	Factorial	0.066	0.7505	0.7579	0.73	0.99
6.	306.90	13.93	0.09	2.5	Factorial	0.124	0.6154	0.5966	0.60	3.04
7.	298.15	17.73	0.13	2	Factorial	0.152	0.8052	0.7807	0.77	3.04
8.	306.90	21.53	0.09	2.5	Factorial	0.459	0.6655	0.6388	0.65	3.99
9.	324.40	21.53	0.16	1.5	Factorial	0.044	0.6904	0.7161	0.73	3.72
10.	315.65	25.33	0.13	2	Factorial	0.272	0.7157	0.6626	0.68	7.41
11.	306.90	13.93	0.09	1.5	Factorial	0.048	0.6804	0.7068	0.70	3.88
12.	333.15	17.73	0.13	2	Factorial	0.045	0.5268	0.5498	0.55	4.37
13.	315.65	17.73	0.13	1	Factorial	0.011	0.8337	0.7990	0.81	4.15
14.	324.40	13.93	0.09	2.5	Factorial	0.103	0.5123	0.4812	0.48	6.05
15.	306.90	21.53	0.16	1.5	Factorial	0.201	0.8059	0.8315	0.83	3.18

16.	315.65	17.73	0.13	2	Factorial	0.180	0.6859	0.6699	0.68	2.32
17.	315.65	10.13	0.13	2	Axial	0.430	0.5703	0.5782	0.58	1.39
18.	315.65	17.73	0.13	2	Axial	0.102	0.6826	0.6699	0.68	1.85
19.	324.40	13.93	0.16	2.5	Axial	0.045	0.5169	0.5637	0.54	8.07
20.	324.40	21.53	0.09	1.5	Axial	0.302	0.6372	0.6336	0.62	0.56
21.	315.65	17.73	0.13	2	Axial	0.043	0.6749	0.6699	0.68	0.73
22.	315.65	17.73	0.05	2	Axial	0.294	0.5594	0.5810	0.57	3.87
23.	315.65	17.73	0.13	2	Axial	0.184	0.6660	0.6699	0.68	0.59
24.	306.90	21.53	0.09	1.5	Axial	0.009	0.7290	0.7490	0.74	2.75
25.	306.90	13.93	0.16	2.5	Center	0.004	0.6352	0.6792	0.64	6.93
26.	315.65	17.73	0.13	2	Center	0.000	0.6815	0.6699	0.68	1.70
27.	306.90	21.53	0.16	2.5	Center	0.000	0.6930	0.7214	0.72	4.10
28.	324.40	13.93	0.16	1.5	Center	0.001	0.7278	0.6739	0.71	7.39
29.	315.65	17.73	0.13	2	Center	0.000	0.6859	0.6699	0.68	2.33
30.	324.40	21.53	0.09	2.5	Center	0.001	0.5257	0.5234	0.54	0.42
									AARD % =	3.23

[a]Standard uncertainties u are u(T) = 1 K, u(P_{CO_2}) = 0.05 kPa, u(m_{BAE}) = 0.001, u(C) = 0.01 mol/L and u(α) = 0.02 mol CO_2/mol amine.

$\alpha_{Predicted}$ = Predicted value of equilibrium CO_2 loading by the RSM software

$$ARD^{*}\ \% = \frac{|Y - \alpha_{cal}|}{Y} \times 100$$

The value of equilibrium CO_2 loading (α_{cal}) was also calculated by the developed model equation (Eq. 3.24). The Microsoft Excel solver software was used to obtain the value of the unknown coefficients involved in Eq. 3.24 corresponding to the RSM experimental sets. The values of unknown coefficients corresponding to RSM-generated data sets are listed in Table B4 of Appendix – B. The AARD % associated with RSM experimental runs were found to be 3.23 %, which is good, reliable, and in the acceptable range.

3.4.11.2 Empirical model validation through RSM software

An empirical model based on T, P_{CO2}, m_{BAE}, and C was developed that correlated α_{cal} with the aforementioned parameters. Eq. 3.24 is the final expression of the developed empirical model in which $a_1$to a_9 be the unknown coefficients and the whole description has been incorporated in section 3.4.3. Based on a defined range of factors, the RSM software created various experimental runs and this software also predicted the value of equilibrium CO_2 loading ($\alpha_{predicted}$) corresponding to these runs. The value of $\alpha_{predicted}$ for the entire experimental run has been reported in Table 3.7. It was found that the value of $\alpha_{predicted}$ was similar to the α_{cal} for all of the experimental runs. Therefore, it can be concluded that based on operating conditions, RSM software validated the empirically developed model. The developed model is highly reliable, and its physical significance has been found in most of the previous works [1,8].

3.4.11.3 Experimental runs validation by quadratic model

Based on factors associated with RSM optimization, a modeling equation was developed by the design-expert software. A, B, C, D, AB, AC, AD, BC, BD, CD, A^2, B^2, C^2, and D^2 were the coefficients involved in the modeling equation. The standard error of these coefficients must be smaller for the model to be perfect. These errors should be similar

within the type of coefficient, i.e., the error from A to D, AB to CD, and A^2 to D^2 remains the same. In this present work, the standard error of coefficients A to D, AB to CD, and A^2 to D^2 was found to be 0.20, 0.25, and 0.19, respectively. Variance inflation factor (VIF) is the measure of multicollinearity related to regression analysis. The ideal value of VIF is 1, and a value greater than 10 indicates that the coefficients were calculated poorly because of multicollinearity. The VIF values of coefficients A, B, C, D, AB, AC, AD, BC, BD, and CD was discovered to be 1, whereas VIF values of A^2, B^2, C^2, and D^2 were found to be 1.05. These coefficients followed the aforementioned conditions of standard error and VIF, and hence a chosen quadratic model was perfect. By analyzing the experimental data, RSM software suggested using linear, 2 FI, and quadratic model but refused to suggest cubic and higher models. The entire experimental runs obtained by opting the CCD design and quadratic model have finally validated the system, and further investigation proceeded.

3.4.11.4 Investigation of ANOVA results

It was essential to focus on the results of ANOVA in order to check the physical significance of the CCD design and quadratic model. Table 3.8 represents the ANOVA results for equilibrium CO_2 loading as a final response for the novel aqueous amine blend of BAE+DMAE. ANOVA analysis provided information on the interaction between the factors in terms of the sum of squares, degree of freedom (df), mean square value, F value, and p-value to examine the validation of the chosen system [1]. If the value of 'Prob > F' is less than 0.050, then the model terms A, B, C, D, and B^2 are significant, and for the present system, it was < 0.0001. When the value of 'Prob > F' exceeds 0.1000, it indicates that the model terms are insignificant. The model's F value of 18.81 suggests that the model is significant. Lack-of-fit value of the system should be insignificant for the model to be

successful. The value of lack-of-fit for the current work was discovered to be 19.57, which was insignificant and reveals the success story of the chosen model. A significant value of lack-of-fit is assumed to be bad, and in that situation, it is mandatory to fit the model. Table 3.9 shows the statistical parameters that were involved in the ANOVA analysis. The statistical parameters included major aspects such as standard deviation, mean, coefficient of variance % (C.V. %), PRESS value, R-squared, adjusted R-squared value, predicted R-squared value, and adequate precision.

The R-squared and adjusted R-squared values represent the model's fitness in terms of the regression line, and the best results are obtained when it is close to 1 [50,89]. The predicted R-squared value gives an idea about the prediction that the regression model makes [50]. The difference between the adjusted-R squared and predicted R-squared values is nearly 0.2, indicating that they are in good agreement. Signal to noise ratio is measured in terms of adequate precision value, and if its value is greater than 4, it is highly desirable for the chosen system [1]. Adequate precision establishes the correlation between the ranges of predicted values of the response to the average prediction error [89]. C.V. % measures the model's reproducibility and is defined as the ratio of the standard value of error to the mean value, which is expressed in percentage. According to the standard, if the value of C.V. % is less than 10, it is highly reproducible [90].

R-squared value, adjusted-R squared, predicted R-squared, and adequate precision, C.V. %, and PRESS value of the present experimental work from ANOVA analysis were found to be 0.9461, 0.8958, 0.6954, and 17.405, 4.28, and 0.068, respectively. All of the ANOVA results indicate that the chosen model and CCD design meet all of the required criteria.

Table 3.8 ANOVA analysis of quadratic model opted in CCD for the calculation of equilibrium CO_2 loading as a final response.

Source	Sum of squares	df	Mean square	F value	p-value Prob > F	
Model	0.21	14	0.015	18.81	< 0.0001	Significant
A: Temperature	0.073	1	0.073	90.84	< 0.0001	
B: Partial pressure of CO_2	0.015	1	0.015	18.70	0.0006	
C: Mole fraction of BAE	0.032	1	0.032	40.17	< 0.0001	
D: Solution concentration	0.079	1	0.079	99.08	< 0.0001	
AB	3.413E-004	1	3.413E-004	0.43	0.5235	
AC	2.698E-004	1	2.698E-004	0.34	0.5700	
AD	6.515E-004	1	6.515E-004	0.81	0.3810	
BC	6.891E-006	1	6.891E-006	8.615E-003	0.9273	
BD	1.280E-003	1	1.280E-003	1.60	0.2252	
CD	2.523E-003	1	2.523E-003	3.15	0.0960	
A^2	9.471E-004	1	9.471E-004	1.18	0.2937	
B^2	3.707E-003	1	3.707E-003	4.64	0.0480	
C^2	2.047E-003	1	2.047E-003	2.56	0.1305	
D^2	3.216E-004	1	3.216E-004	0.40	0.5356	
Residual	0.012	15	7.998E-004			
Lack of Fit	0.012	10	1.170E-003	19.57	0.0021	Non-significant
Pure Error	2.989E-004	5	5.979E-005			
Cor Total	0.22	29				

Table 3.9 Statistical parameters obtained from the analysis of variance (ANOVA) for the modelling of equilibrium CO_2 loading as a final response.

Standard deviation	0.028
Mean	0.66
C.V. %	4.28
PRESS	0.068
R-squared	0.9461
Adj R-squared	0.8958
Pred R-square	0.6954
Adeq precision	17.405

3.4.11.5 RSM modeling

The model equation consisting of the final response (Y) based on experimental run sets generated by RSM software can be represented as follows:

$$Y = 0.68 - 0.055\,A + 0.025\,B + 0.037\,C - 0.057\,D - 0.004619\,AB + 0.004106\,AC - 0.006381\,AD + 0.0006563\,BC + 0.008944\,BD - 0.013\,CD - 0.005876\,A^2 - 0.012\,B^2 - 0.008639\,C^2 + 0.003424\,D^2 \quad (3.30)$$

Where A, B, C, and D denote the coded value of temperature, CO_2 partial pressure, mole fraction of BAE, and solution concentration, respectively. Figure 3.10 (a) represents the relationship between the predicted and actual values of the final response (Y). Using a quadratic model, the actual and predicted data sets were plotted in a straight line, and the predicted values were in good agreement with the actual values. Eq. 3.30 is the RSM

modeling equation that correlates the interaction amongst the independent variables and finally provides the response.

After ANOVA analysis, diagnostics tool in RSM software were considered for further investigation, and residual values were targeted. The residuals are defined as the difference between the predicted and the observed value by utilizing different factors involved in the system [90]. Results of residuals were reported in terms of studentized residual, which is defined as the ratio of residuals to the standard deviation. The residual plots are helpful in validating the model that is used to estimate the final response. Figure 3.10 (b) shows the normal plot of residuals; it is a correlation between normal % probability vs. internally studentized residuals. The residuals were perfectly distributed along a straight line, indicating a strong relationship between the experimental and predicted values. This straight line signifies the normal distribution of errors that took place. Figure 3.10 (c) shows the relationship between the residuals vs. the predicted value of the response. It was a correlation that was plotted between the predicted value (i.e., X-axis) and internally studentized residuals (i.e., Y-axis). The residuals acquired the constant variance, which is a clear validation of the model [1,50,58]. Figure 3.10 (d) shows the relationship between the residuals vs. run number for the estimation of equilibrium CO_2 loading. It was the random plot that did not follow any specific pattern between the run number and the internally studentized residuals [55]. When considering the internally studentized residuals, it is clear from Figure 3.10 (b), (c), and (d) that the data points were distributed within the range of -3.00 to + 3.00. Based on the findings of the entire investigation, the CCD design with a quadratic model passes all statistical tests.

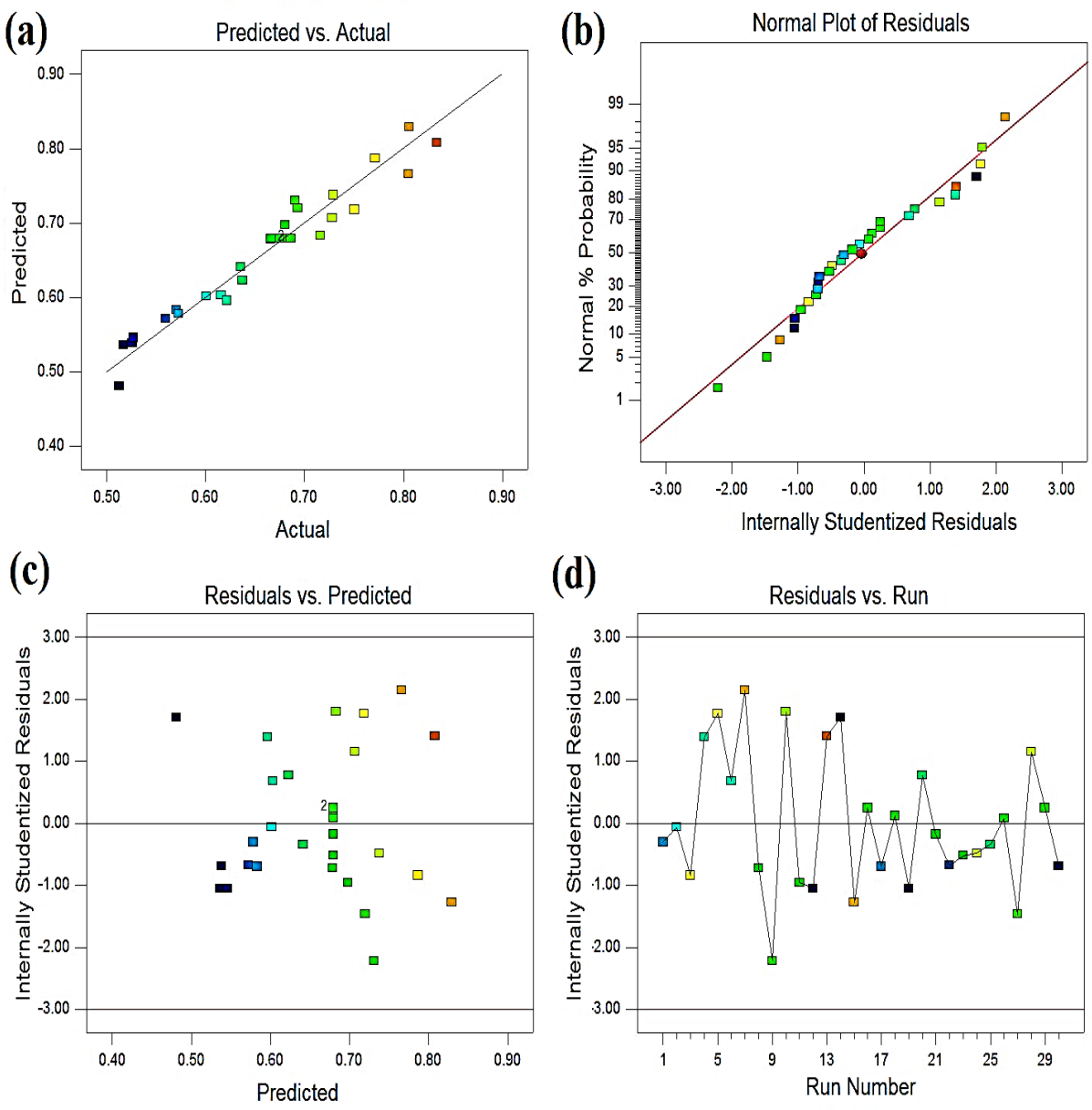

Figure 3.10 (a) Correlation between the predicted vs. actual values of equilibrium CO_2 loading as a final response; (b) Normal plot of residuals showing the relationship between the normal % probability vs. internally studentized residuals; (c) Correlation between the internally studentized residuals vs. predicted values of equilibrium CO_2 loading as a final response; (d) Relationship between the internally studentized residuals vs. the run number.

3.4.11.6 Investigation on 3-D surfaces and contour graphs

3-D surfaces and contour graphs represent the effect of independent variables on equilibrium CO_2 loading as a final response [54,55]. These surface and contour representations locate all the independent variables at a specific point to provide information on optimum response. These 3-D surfaces and contour graphs are graphical representations of the model chosen for the entire study [1,50]. Figure 3.11 (a) and (b) are the 3-D surface, and the contour representation of temperature (A) and CO_2 mole fraction (B) and their behavior on equilibrium CO_2 loading as a final response has been shown. These representations suggested that the final response of equilibrium CO_2 loading was maximum at the low temperature and vice-versa. This is due to the known fact that at high temperature, the equilibrium shifts in the reverse direction, and at high temperature, desorption of gas also takes place. Therefore, the solubility of gas decreases as the temperature increases. A complete description of the effect of temperature on equilibrium CO_2 loading is incorporated in section 3.4.2.1. Similarly, the response was increased as the CO_2 partial pressure value increased from a lower value to a higher value. Solubility of gas in the liquid follows Henry's law, and when more molecules of CO_2 are available in the liquid, then solubility of CO_2 gas increases in the aqueous amine blend. The complete description of the effect of CO_2 partial pressure on equilibrium CO_2 loading has been incorporated in section 3.4.2.2. Based on the aforementioned explanation, the interaction between the factors 'A' and 'B' suggested that at low temperature and high CO_2 partial pressure, the value of equilibrium CO_2 loading was maximum. Figure 3.11 (c) and (d) represent the behavior of temperature (A) and mole fraction of BAE (C) on the final response.

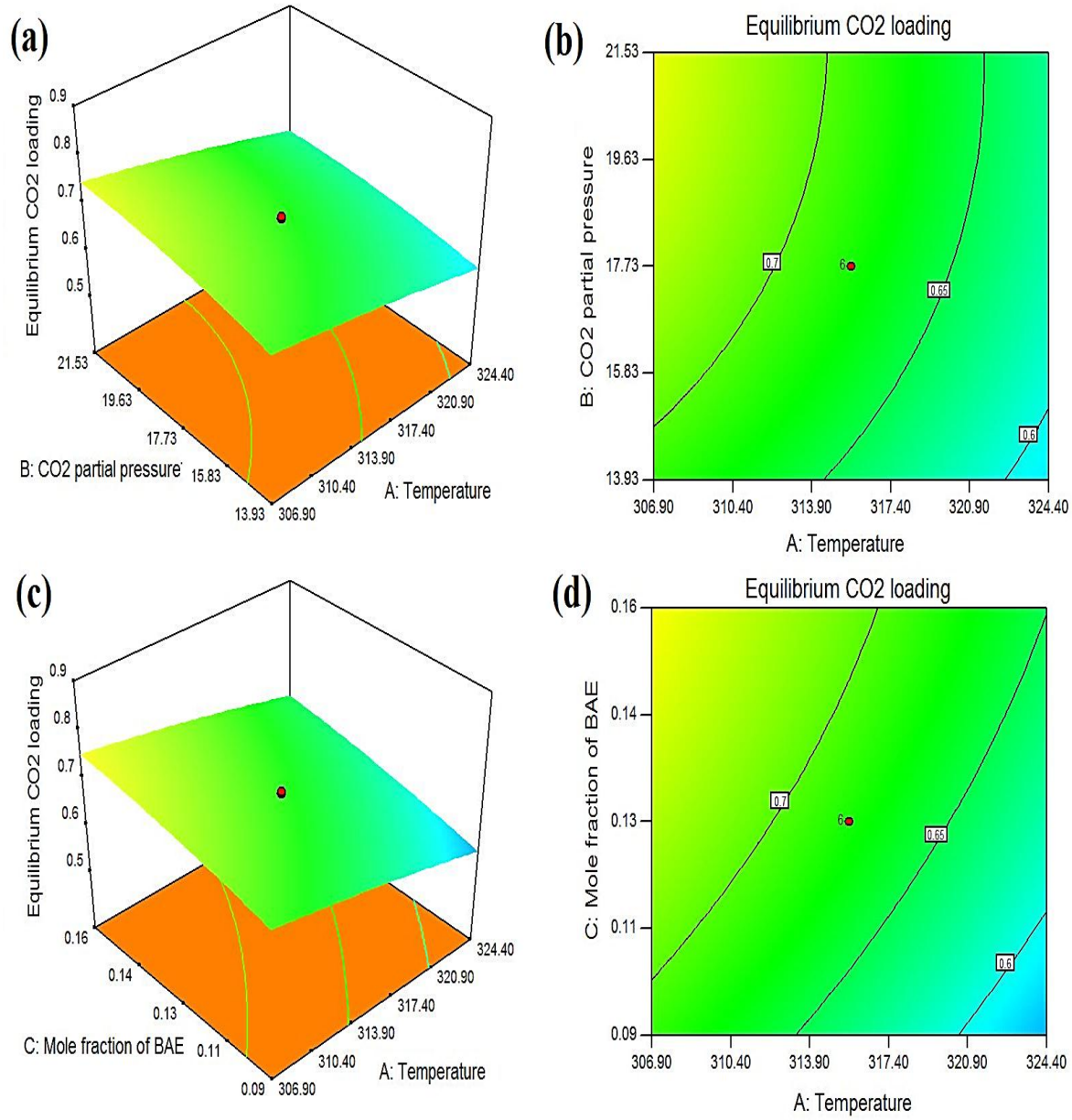

Figure 3.11 (a) 3-D surface showing the effect of temperature (A) and CO_2 partial pressure (B) on final response; (b) Contour graph representing the effect of temperature (A) and CO_2 partial pressure (B) on final response; (c) 3-D surface showing the effect of temperature (A) and mole fraction of BAE (C) on final response; (d) Contour graph representing the effect of temperature (A) and mole fraction of BAE (C) on final response.

3-D plots and contour graphs of these representations indicated that as the mole fraction of BAE in the solution increased, the response increased. BAE has a strong tendency to form bicarbonate and carbonate resulting in a large amount of equilibrium CO_2 loading in the aqueous amine blend. The entire description of the effect of the mole fraction of BAE on the CO_2 loading has been incorporated in section 3.4.2.3. Based on the effects of interaction between the factors 'A' and 'C' on equilibrium CO_2 loading, it is concluded that at low temperature and high mole fraction of BAE provided the optimum value of equilibrium CO_2 loading.

Figure 3.12 (a) and (b) represent the 3-D plot and contour graph of temperature (A) and solution concentration (D) and their effect on the final response. These figures conclude that the response is maximum at low solution concentration and vice-versa. The steric hindrance of the solution increases as the solution concentration of the aqueous amine blend increases, creating a barrier in the conversion of carbamate to bicarbonate. The whole description of the effect of solution concentration on equilibrium CO_2 loading has been incorporated in section 3.4.2.4. The effect of interaction between the factors 'A' and 'D' on equilibrium CO_2 loading, it is concluded that at low temperature and low solution concentration, the optimum value of response has been obtained. Similarly, Figure 3.12 (c) and (d) represent the 3-D plot and contour graph of CO_2 partial pressure (B) and mole fraction of BAE (C) and their effect on the final response. It is concluded that on the interaction between the factors 'B' and 'C', the maximum response can be obtained at high CO_2 partial pressure and high mole fraction of BAE in the entire solution.

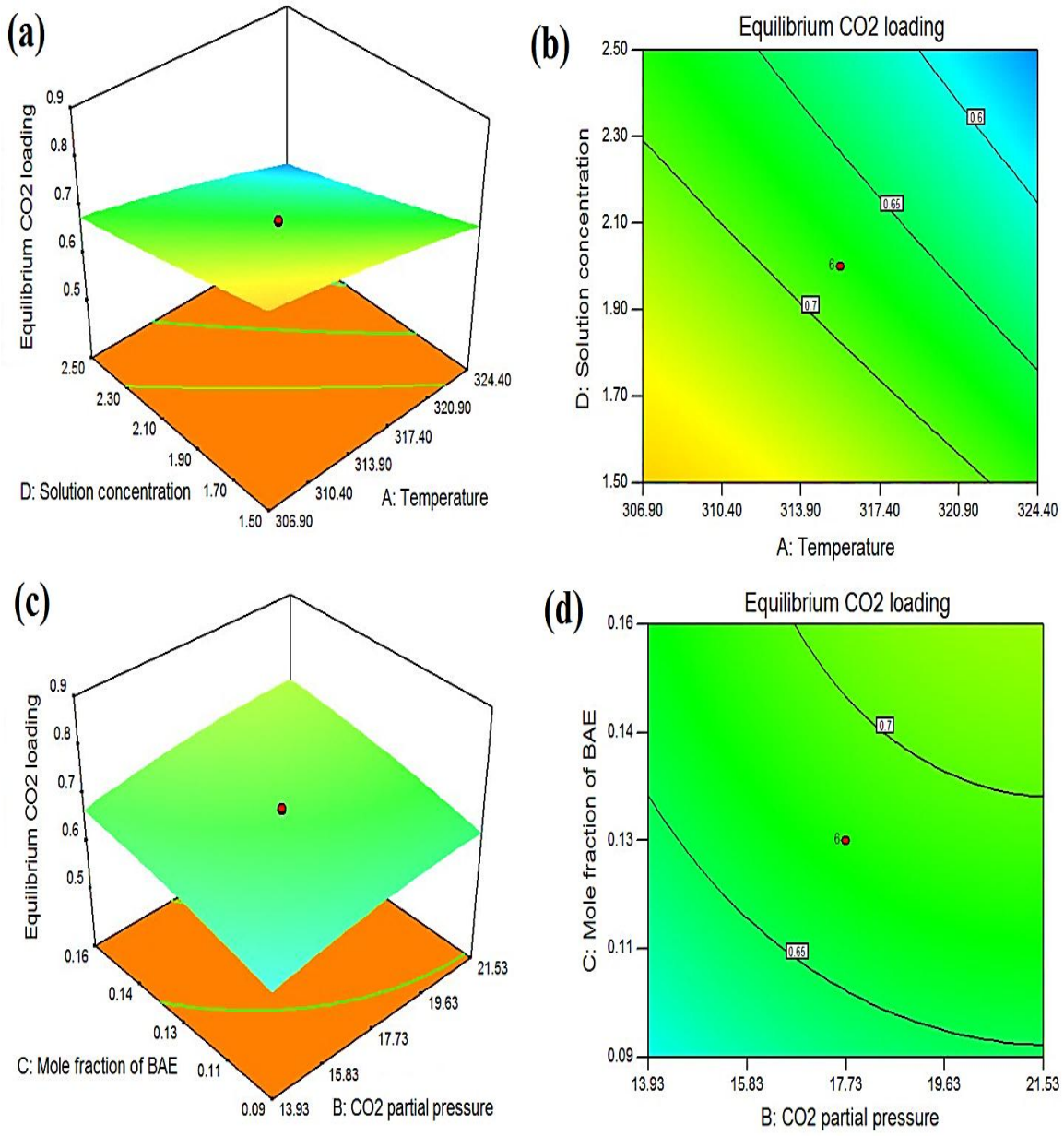

Figure 3.12 (a) 3-D surface showing the effect of temperature (A) and solution concentration (D) on final response; (b) Contour graph representing the effect of temperature (A) and solution concentration (D) on final response; (c) 3-D surface showing the effect of CO_2 partial pressure (B) and mole fraction of BAE (C) on final response; (d) Contour graph representing the effect of CO_2 partial pressure (B) and mole fraction of BAE (C) on final response.

Figure 3.13 (a) and (b) represent the 3-D plots and contour graphs of CO_2 partial pressure (B) and solution concentration (D) and their interaction effect on equilibrium CO_2 loading. Interaction between the factors 'B' and 'D', it is concluded that at low solution concentration in the aqueous amine blend and high CO_2 partial pressure, the maximum value of response was obtained. Likewise, the interaction between the mole fraction of BAE (C) and solution concentration (D) has been shown in Figure 3.13 (c) and (d). It is concluded that at a high mole fraction of BAE in the solution and low solution concentration, the optimum value of response has been found.

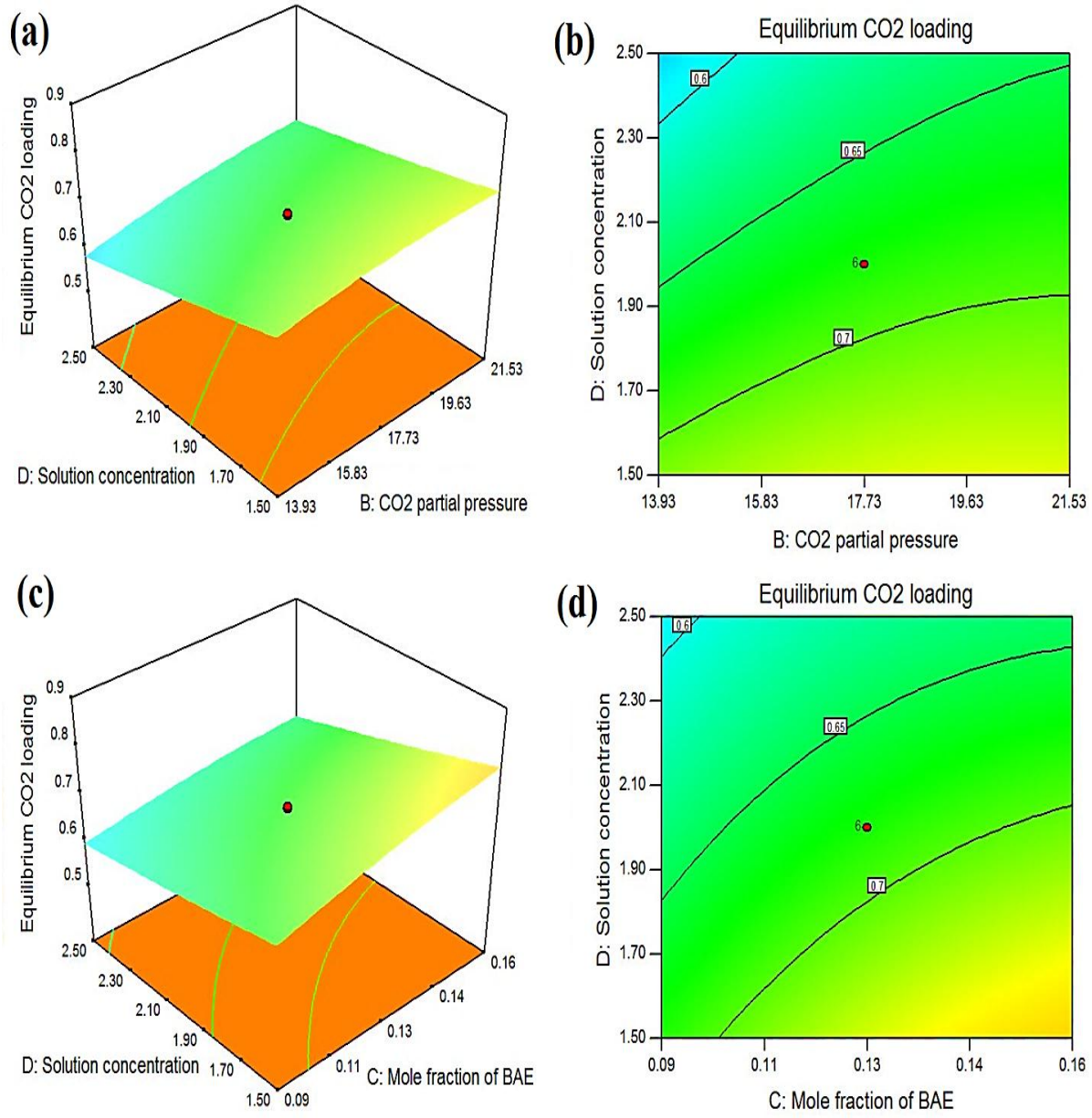

Figure 3.13 (a) 3-D surface showing the effect of CO_2 partial pressure (B) and solution concentration (D) on final response; (b) Contour graph representing the effect of CO_2 partial pressure (B) and solution concentration (D) on final response; (c) 3-D surface showing the effect of mole fraction of BAE (C) and solution concentration (D) on final response; (d) Contour graph representing the effect of mole fraction of BAE (C) and solution concentration (D) on final response.

3.4.11.7 Optimum value prediction and its validation by the RSM

After analyzing the behavior of the independent variable on equilibrium CO_2 loading in the form of 3-D plots and contour graphs, then it was essential to obtain the optimized results. In the RSM software's numerical optimization section, it was necessary to set a goal for each of the independent variables, and then the best results were obtained. For the entire independent variables, the goal was set to be in range while the equilibrium CO_2 loading was set to maximum. Since the equilibrium CO_2 loading was the only response, therefore it was assigned to the five importance level, while the rest of the other independent variables provided three importance level that was already set as default in the RSM software. Table 3.10 shows the desired goal and importance of the input and output variables. Ramps data in the numerical optimization section of the RSM software provided the optimum values for all factors and also predicted the maximum equilibrium CO_2 loading as a final response, as shown in Figure 3.14. It has predicted optimum condition at temperature (A) = 306.90 K, CO_2 partial pressure (B) = 21.22 kPa, mole fraction of BAE (C) = 0.16, solution concentration (D) = 1.50 mol/L, and equilibrium CO_2 loading = 0.829265 mol CO_2/mol amine. Desirability is defined as the objective function, which is composed of factors that are involved in the entire system. The objective function must be maximized, and the value of desirability lies between 0 to 1. For this present work, the desirability of the system was found to be 0.986, which is much closer to 1.

Table 3.10 Numerical solutions, goal, lower and upper limits of the factors to calculate the overall desirability of the system.

Factors	Goal	Lower limit	Upper limit	Lower weight	Upper weight	Importance
A: Temperature	In range	306.90	324.40	1	1	3
B: CO_2 partial pressure	In range	13.93	21.53	1	1	3
C: Mole fraction of BAE	In range	0.0875	0.1625	1	1	3
D: Solution concentration	In range	1.5	2.5	1	1	3
Equilibrium CO_2 loading	Maximize	0.5123	0.8337	1	1	5

It was important to validate the optimum prediction made by the RSM software. Two different experiments were performed on the lab scale to validate the predicted results. The operating conditions of temperature, CO_2 partial pressure, and mole fraction of CO_2 were the same as in the case of predicted values. However, a small change in the solution concentration of the BAE+DMAE aqueous amine blend was made, and the results were compared to the predicted values. Experiment 1st : T = 306.90 K, P_{CO2} = 21.22 kPa, m_{BAE} = 0.16, and C = 1.40 mol/L. Experiment 2nd : T = 306.90 K, P_{CO2} = 21.22 kPa, m_{BAE} = 0.16, and C = 1.60 mol/L.

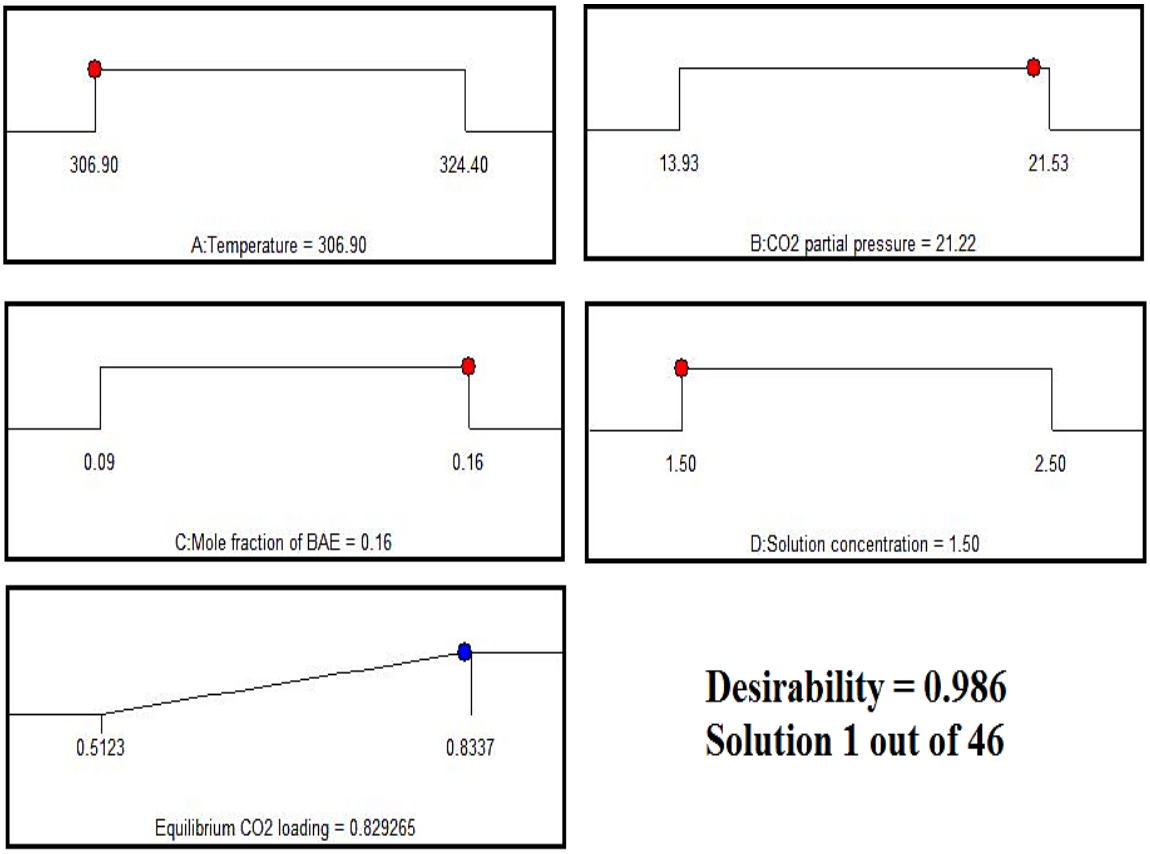

Figure 3.14 Desirability ramp, optimum values of factors and equilibrium CO_2 loading as a final response in numerical optimization.

Table 3.11 shows the operating conditions of the actual experimental runs and the predicted run, as well as their final responses. Based on these experimental runs, the value of equilibrium CO_2 loading for experiments 1st and 2nd was found to be 0.830492 mole CO_2/mol amine and 0.814383 mol CO_2/mol amine. The average value of the equilibrium CO_2 loading of these experimental runs was found to be 0.822437 mol CO_2/mol amine. This value of the final response was less than 1 % of the predicted value. So, it can be concluded that the experimental results validate the predicted value. Therefore, the chosen CCD design and quadratic model were perfect and validated the entire study of optimization.

Table 3.11 RSM predicted value vs. actual experimental value.

	Temperature (K)	**CO_2 partial pressure (kPa)**	**Mole fraction of BAE**	**Solution concentration (mol/L)**	**Equilibrium CO_2 loading (Response, Y)**
Experimental value	306.90	21.22	0.16	1.40	0.830492
Predicted value	306.90	21.22	0.16	1.50	0.829265
Experimental value	306.90	21.22	0.16	1.60	0.814383

3.5 Conclusions

In this study, a novel aqueous amine blend of BAE and DMAE was prepared, and this blend performed admirably in terms of CO_2 absorption and desorption performance. The pH investigation concluded that the pH of the CO_2-unloaded, CO_2-loaded, and CO_2-regenerated amine blend lay in the range of 12.01–12.30, 8.71–9.64, and 10–11, respectively. The CO_2 absorption experiments were carried out at temperature (T) ranging from 298.15–333.15 K, CO_2 partial pressure (P_{CO2}) ranged from 10.13–25.33 kPa, mole fraction of BAE (m_{BAE}) changed from 0.05–0.20, and solution concentration (C) varied from 1–3 mol/L. Absorption investigation revealed that the value of equilibrium CO_2 loading increased with an increase in CO_2 partial pressure and also increased with an increase in the mole fraction of BAE in the aqueous amine blend of BAE+DMAE. However, the equilibrium CO_2 loading decreased with an increase in temperature and solution concentration of the aqueous amine blend. The absorption study on 37 experimental runs provided the maximum value of equilibrium CO_2 loading of 0.9365 mol CO_2/mol amine at T = 313.15 K, P_{CO2} = 25.33 kPa, m_{BAE} = 0.20, and C = 1 mol/L. The absorption time has also been shown to have a significant effect on CO_2 loading. The absorption rate was initially fast in relation to time, but it gradually slowed until it reached the condition of equilibrium CO_2 loading at the longest absorption time. An empirical model was developed that validated the experimental results, and a reliable % AARD was found to be 3.41 %. CO_2 chemically reacted with the aqueous amine blend, and the intermediate products were produced and characterized by ^{13}C NMR and FTIR techniques. For ^{13}C NMR analysis, for the CO_2-unloaded sample, the peaks of BAE have obtained at 13.84–31.03 ppm, whereas the peak at 44.72–60.18 ppm signifies the presence of DMAE

in the BAE+DMAE amine blend. Intermediate complexes of $BAEH^+$ and $DMAEH^+$ in CO_2-loaded amine samples showed peaks at 13.47–27.87 ppm and 43.49–61.20 ppm, respectively. CO_2-regenerated amine blend showed BAE and DMAE peaks at 13.58–30.59 ppm and 44.46–59.86 ppm, respectively. Similarly, FTIR analysis revealed the presence of BAE and DMAE peaks in the CO_2-loaded and CO_2-regenerated samples, whereas this technique also revealed intermediate complexes formed in the CO_2-loaded samples.

The desorption study concluded that the cyclic equilibrium CO_2 loading of 3 mol/L of BAE+DMAE amine blend was 0.6176 mol CO_2/L.solution. The cyclic capacity of the BAE+DMAE amine blend at C = 3 mol/L demonstrated 71.23 % higher cyclic capacity than conventional 30 wt% MEA. The heat duty for 1 mol/L, 2 mol/L, and 3 mol/L solutions was found to be 288.55 kJ/mol CO_2, 177.31 kJ/mol CO_2, and 112.96 kJ/mol CO_2. As compared with conventional MEA, this heat duty value was reduced by 35.87 %, 60.59 %, and 74.89 % for 1 mol/L, 2 mol/L, and 3 mol/L, respectively. The molar ratio of BAE in the aqueous amine blend also showed a significant effect on heat duty and its value increased as the molar ratio of BAE in the aqueous amine blend increased. The regeneration efficiency of 1 mol/L, 2 mol/L, and 3 mol/L solutions of the BAE+DMAE amine blend was found to be 77.45 %, 75.15 %, and 83.27 %, respectively. The heat of CO_2 absorption of this novel aqueous amine blend was found to be -72.74 kJ/mol. This ΔH_{abs} value recommends this novel aqueous blend for industrial purposes since this value is higher than tertiary amines but lower than primary amines. BAE and DMAE toxicity testing revealed that these amines were slightly toxic, with LD_{50} values of 890 mg/kg and 2000 mg/kg, respectively. These amines and their blend impart the least hazardous impact on the environment and are highly recommended for future industrial applications. Finally,

optimization of this present work was done with the help of RSM software. CCD design and quadratic model developed a modeling equation in which equilibrium CO_2 loading was the final response. The chosen model passed all the necessary criteria. The model was significant, the lack of fit was non-significant, and the values of the ANOVA analyses were within an acceptable range, confirming the validity of the experiments. RSM software predicted the optimum equilibrium CO_2 loading of 0.829265 mol CO_2/mol amine at T = 306.90 K, P_{CO2} = 21.22 kPa, m_{BAE} = 0.16, and C = 1.5 mol/L. On considering the major aspects of this study, it can be recommended that this novel aqueous amine blend of BAE+DMAE is highly suitable for industrial application.

ASSOCIATED CONTENT

Appendix – A and Appendix – B

Figure A6 related to this chapter, can be found in Appendix–A.

Table B3 and Table B4**,** related to this chapter, can be found in Appendix–B.

References

[1] Gautam A, Kumar Mondal M, 2023. Post-combustion capture of CO_2 using novel aqueous Triethylenetetramine and 2-Dimethylaminoethanol amine blend: Equilibrium CO_2 loading-empirical model and optimization, CO_2 desorption, absorption heat, and ^{13}C NMR analysis. Fuel. 331, 125864. https://doi.org/10.1016/j.fuel.2022.125864.

[2] Gautam A, Mondal MK, 2023. Review of recent trends and various techniques for CO_2 capture: Special emphasis on biphasic amine solvents. Fuel. 334, 126616. https://doi.org/10.1016/j.fuel.2022.126616.

[3] Agnihotri N, Gupta GK, Mondal MK. Thermo-kinetic analysis, thermodynamic parameters and comprehensive pyrolysis index of Melia azedarach sawdust as a genesis of bioenergy. Biomass Conv Bioref 2024;14:1863–80. https://doi.org/10.1007/s13399-022-02524-y.

[4] Wang R, Zhao H, Wang Y, Qi C, Zhang S, Wang L, Li M, 2022. Development of biphasic solvent for CO_2 capture by tailoring the polarity of amine solution. Fuel. 325, 124885. https://doi.org/10.1016/j.fuel.2022.124885.

[5] Ahmed RE, Wiheeb AD. Enhancement of carbon dioxide absorption into aqueous potassium carbonate by adding amino acid salts. Mater Today Proc 20:2020;611-6. https://doi.org/10.1016/j.matpr.2019.09.198.

[6] Agnihotri N, Mondal MK, 2023. Comparison of non-catalytic and in-situ catalytic pyrolysis of Melia azedarach sawdust. J Anal Appl Pyrolysis 172, 106006. https://doi.org/10.1016/j.jaap.2023.106006.

[7] Kim J, Lee J, Lee Y, Kim H, Kim E, Lee KS, 2019. Evaluation of aqueous polyamines as CO_2 capture solvents. Energy. 187, 115908. https://doi.org/10.1016/j.energy.2019.115908.

[8] Pandey D, Kumar Mondal M, 2021. Thermodynamic modeling and new experimental CO_2 solubility into aqueous EAE and AEEA blend, heat of absorption, cyclic absorption capacity and desorption study for post-combustion CO_2 capture. Chem Eng J 410, 128334. https://doi.org/10.1016/j.cej.2020.128334.

[9] Xiao M, Liu H, Gao H, Liang Z. Liang. CO_2 absorption with aqueous tertiary amine solutions: Equilibrium solubility and thermodynamic modeling. J Chem Thermodyn 2018;122:170–82. https://doi.org/10.1016/j.jct.2018.03.020.

[10] Chowdhury FA, Okabe H, Shimizu S, Onoda M, Fujioka Y. Development of novel tertiary amine absorbents for CO_2 capture. Energy Procedia 2009;1:1241–8. https://doi.org/10.1016/j.egypro.2009.01.163.

[11] Kim YE, Park JH, Yun SH, Nam SC, Jeong SK, Yoon Yi. Carbon dioxide absorption using a phase transitional alkanolamine – alcohol mixture. J Ind Eng Chem 2014;20:1486–92. https://doi.org/10.1016/j.jiec.2013.07.036.

[12] Lv B, Guo B, Zhou Z, Jing G. Mechanisms of CO_2 capture into monoethanolamine solution with different CO_2 loading during the absorption/desorption processes. Environ Sci Technol 2015;49:10728–35. https://doi.org/10.1021/acs.est.5b02356.

[13] Muchan P, Saiwan C, Narku-Tetteh J, Idem R, Supap T, Tontiwachwuthikul P. Screening tests of aqueous alkanolamine solutions based on primary, secondary, and tertiary structure for blended aqueous amine solution selection in post combustion CO_2 capture. Chem Eng Sci 2017;170:574–82. https://doi.org/10.1016/j.ces.2017.02.031.

[14] Huang Q, Jing G, Zhou X, Lv B, Zhou Z. A novel biphasic solvent of amino-functionalized ionic liquid for CO_2 capture: High efficiency and regenerability. J CO_2 Util 2018;25:22–30.https://doi.org/10.1016/j.jcou.2018.03.001.

[15] Ji L, Yu H, Li K, Yu B, Grigore M, Yang Q, et al. Integrated absorption-mineralisation for low-energy CO_2 capture and sequestration. Appl Energy 2018;225:356–66. https://doi.org/10.1016/j.apenergy.2018.04.108.

[16] Chen M, Li M, Zhang F, Hu X, Wu Y. Fast and Efficient CO_2 Absorption in Non-aqueous Tertiary Amines Promoted by Ethylene Glycol. Energy Fuels 2022;36:4830–6. https://doi.org/10.1021/acs.energyfuels.2c00215.

[17] Gao G, Li X, Jiang W, Zhao Z, Xu Y, Wu F, Luo C, Zhang L, 2022. Improved quasi-cycle capacity method based on microcalorimetry strategy for the fast screening of amino acid salt absorbents for CO_2 capture. Sep Purif Technol 289, 120767. https://doi.org/10.1016/j.seppur.2022.120767.

[18] Zhou X, Liu F, Lv B, Zhou Z, Jing G. Evaluation of the novel biphasic solvents for CO_2 capture: Performance and mechanism. Int J Greenh Gas Control 2017;60:120–8. https://doi.org/10.1016/j.ijggc.2017.03.013.

[19] Agnihotri N, Mondal MK, 2023. Thermal analysis, kinetic behavior, reaction modeling, and comprehensive pyrolysis index of soybean stalk pyrolysis. Biomass Conv Bioref. https://doi.org/10.1007/s13399-023-03807-8.

[20] Kumar S, Padhan R, Mondal MK. Equilibrium solubility of CO_2 in aqueous blend of 2-(diethylamine) ethanol and 2-(2-aminoethylamine) ethanol. J Chem Eng Data 2018;63:1163-9. https://doi.org/10.1021/acs.jced.7b00544.

[21] Kumar S, Mondal MK. Equilibrium solubility measurement and modeling of CO_2 absorption in aqueous blend of 2-(diethyl amino) ethanol and ethylenediamine. J Chem Eng Data 2020;65:523-31. https://doi.org/10.1021/acs.jced.9b00699.

[22] Kumar S, Mondal MK. Selection of efficient absorbent for CO_2 capture from gases containing low CO_2. Korean J Chem Eng 2020;37:231–9. https://doi.org/10.1007/s11814-019-0440-6

[23] Perumal M, Jayaraman D, Balraj A. Selection of efficient absorbent for CO_2 capture from gases containing low CO_2. Korean J Chem Eng 2020;37:231-9. https://doi.org/10.1007/s11814-019-0440-6.

[24] Li T, Yang C, Tantikhajorngosol P, Sema T, Shi H, Tontiwachwuthikul P, 2021. Experimental studies on CO_2 absorption and solvent recovery in aqueous blends of monoethanolamine and tetrabutylammonium hydroxide. Chemosphere. 276, 130159. https://doi.org/10.1016/j.chemosphere.2021.130159.

[25] Pandey D, Mondal MK, 2020. Equilibrium CO_2 solubility in the aqueous mixture of MAE and AEEA: Experimental study and development of modified thermodynamic model. Fluid Phase Equilib. 522, 112766. https://doi.org/10.1016/j.fluid.2020.112766.

[26] Singh S, Pandey D, Mondal MK. New Experimental Data on Equilibrium CO_2 Loading into Aqueous 3-Dimethyl Amino-1-propanol and 1,5-Diamino-2-methylpentane Blend: Empirical Model and CO_2 Absorption Enthalpy. J Chem Eng Data 2021;66:740–8. https://doi.org/10.1021/acs.jced.0c00851.

[27] Zhang R, He X, Liu T, Li C, Xiao M, Ling H, Hu X, Zhang X, Tang F, Luo HA, 2022. Thermodynamic studies for improving the prediction of CO_2 equilibrium solubility in

aqueous 2-dimethylamino-2-methyl-1-propanol. Sep Purif Technol 295, 121292. https://doi.org/10.1016/j.seppur.2022.121292.

[28] Machida H, Oba K, Tomikawa T, Esaki T, Yamaguchi T, Horizoe H. Development of phase separation solvent for CO_2 capture by aqueous (amine + ether) solution. J Chem Thermodyn 2017;113:64–70. https://doi.org/10.1016/j.jct.2017.05.043.

[29] Ping T, Dong Y, Shen S. Shen, Energy-efficient CO_2 capture using nonaqueous absorbents of secondary alkanolamines with a 2-butoxyethanol cosolvent. ACS Sustain Chem Eng 2020;8:18071–82. https://doi.org/10.1021/acssuschemeng.0c06345.

[30] Dong Y, Ping T, Shen S. Solubility of CO_2 in nonaqueous system of 2-(butylamino) ethanol with 2-butoxyethanol: Experimental data and model representation. Chinese J Chem Eng 2022;41:441–8. https://doi.org/10.1016/j.cjche.2021.11.003.

[31] Ping T, Dong Y, Shen S, 2020. Densities, viscosities and spectroscopic study of partially CO_2-loaded nonaqueous blends of 2-butoxyethanol with 2-(ethylamino) ethanol and 2-(butylamino) ethanol at temperatures of (293.15 to 353.15) K. J Mol Liq 312, 113389. https://doi.org/10.1016/j.molliq.2020.113389.

[32] Liang ZH, Rongwong W, Liu H, Fu K, Gao H, Cao F, Zhang R, Sema T, Henni A, Sumon K, Nath D. Recent progress and new developments in post-combustion carbon-capture technology with amine based solvents. Int J Greenh Gas Control 2015;40:26-54. https://doi.org/10.1016/j.ijggc.2015.06.017.

[33] El Hadri N, Quang DV, Goetheer ELV, Abu Zahra MRM. Aqueous amine solution characterization for post-combustion CO_2 capture process. Appl Energy 2017;185:1433-49. https://doi.org/10.1016/j.apenergy.2016.03.043.

[34] Wai SK, Saiwan C, Idem R, Supap T, Nwaoha C. Carbon Dioxide (CO_2) Solubility in Diethylenetriamine and 2-Amino-2-Methyl-1-Proponal (DETA-AMP) Solvent System for Amine-Based CO_2 Capture in Flue Gas from Coal Combustion. Energy Procedia 2017;114:1973–9. https://doi.org/10.1016/j.egypro.2017.03.1329.

[35] Liu H, Li M, Idem R, (PT) Tontiwachwuthikul P, Liang Z. Analysis of solubility, absorption heat and kinetics of CO_2 absorption into 1-(2-hydroxyethyl)pyrrolidine solvent. Chem Eng Sci 2017;162:120–30. https://doi.org/10.1016/j.ces.2016.12.070.

[36] Aronu UE, Gondal S, Hessen ET, Haug-Warberg T, Hartono A, Hoff KA, et al. Solubility of CO_2 in 15, 30, 45 and 60 mass% MEA from 40 to 120 °C and model representation using the extended UNIQUAC framework. Chem Eng Sci 2011;66:6393–406. https://doi.org/10.1016/j.ces.2011.08.042.

[37] Barzagli F, Mani F, Peruzzini M. A Comparative Study of the CO_2 Absorption in Some Solvent-Free Alkanolamines and in Aqueous Monoethanolamine (MEA). Environ Sci Technol 2016;50:7239–46. https://doi.org/10.1021/acs.est.6b00150.

[38] Afari DB, Coker J, Narku-Tetteh J, Idem R. Comparative Kinetic Studies of Solid Absorber Catalyst (K/MgO) and Solid Desorber Catalyst (HZSM-5)-Aided CO_2 Absorption and Desorption from Aqueous Solutions of MEA and Blended Solutions of BEA-AMP and MEA-MDEA. Ind Eng Chem Res 2018;57:15824–39. https://doi.org/10.1021/acs.iecr.8b02931.

[39] Srisang W, Pouryousefi F, Osei PA, Decardi-Nelson B, Akachuku A, Tontiwachwuthikul P, Idem R. Evaluation of the heat duty of catalyst-aided amine-based post combustion CO_2 capture. Chem Eng Sci 2017;170:48–57. https://doi.org/10.1016/j.ces.2017.01.049.

[40] Cao F, Gao H, Xiong Q, Liang Z. Experimental studies on mass transfer performance for CO_2 absorption into aqueous N,N-dimethylethanolamine (DMEA) based solutions in a PTFE hollow fiber membrane contactor. Int J Greenh Gas Control 2019;82:210–7. https://doi.org/10.1016/j.ijggc.2018.12.011.

[41] Ling H, Gao H, Liang Z. Comprehensive solubility of N_2O and mass transfer studies on an effective reactive N,N-dimethylethanolamine (DMEA) solvent for post-combustion CO_2 capture. Chem Eng J 2019;355:369–79.https://doi.org/10.1016/j.cej.2018.08.147.

[42] Nwaoha C, Saiwan C, Supap T, Idem R, Tontiwachwuthikul P, Rongwong W, et al. Carbon dioxide (CO_2) capture performance of aqueous tri-solvent blends containing 2-amino-2-methyl-1-propanol (AMP) and methyldiethanolamine (MDEA) promoted by diethylenetriamine (DETA). Int J Greenh Gas Control 2016;53:292–304. https://doi.org/10.1016/j.ijggc.2016.08.012.

[43] Hwang SJ, Kim J, Kim H, Lee KS. Solubility of Carbon Dioxide in Aqueous Solutions of Three Secondary Amines: 2-(Butylamino)ethanol, 2-(Isopropylamino)ethanol, and 2-(Ethylamino)ethanol Secondary Alkanolamine Solutions. J Chem Eng Data 2017;62:2428–35. https://doi.org/10.1021/acs.jced.7b00364.

[44] Barzagli F, Giorgi C, Mani F, Peruzzini M. Reversible carbon dioxide capture by aqueous and non-aqueous amine-based absorbents: A comparative analysis carried out by ^{13}C NMR spectroscopy. Appl Energy 2018;220:208–19. https://doi.org/10.1016/j.apenergy.2018.03.076.

[45] Xiao M, Cui D, Liu H, Tontiwachwuthikul P, Liang Z. A new model for correlation and prediction of equilibrium CO_2 solubility in N-methyl-4-piperidinol solvent. AIChE J 2017;63:3395-403. https://doi.org/10.1002/aic.15709.

[46] Zheng W, Yan Z, Zhang R, Jiang W, Luo X, Liang Z, Yang Q, Yu H, 2022. A study of kinetics, equilibrium solubility, speciation and thermodynamics of CO_2 absorption into benzylamine (BZA) solution. Chem Eng Sci. 251, 117452. https://doi.org/10.1016/j.ces.2022.117452.

[47] Narku-Tetteh J, Muchan P, Saiwan C, Supap T, Idem R. Selection of components for formulation of amine blends for post combustion CO_2 capture based on the side chain structure of primary, secondary and tertiary amines. Chem Eng Sci 2017;170:542–60. https://doi.org/10.1016/j.ces.2017.02.036.

[48] Ramezani R, Mazinani S, Di Felice R. Density, Viscosity, pH, Heat of Absorption, and CO_2 Loading Capacity of Methyldiethanolamine and Potassium Lysinate Blend Solutions. J Chem Eng Data 2021;66:1611–29. https://doi.org/10.1021/acs.jced.0c00855.

[49] Gadaleta D, Vuković K, Toma C, Lavado GJ, Karmaus AL, Mansouri K, Kleinstreuer NC, Benfenati E, Roncaglioni A. SAR and QSAR modeling of a large collection of LD_{50} rat acute oral toxicity data. J Cheminform 2019;11:1-6. https://doi.org/10.1186/s13321-019-0383-2.

[50] Asgarifard P, Rahimi M, Tafreshi N. Response surface modelling of CO_2 capture by ammonia aqueous solution in a microchannel. Can J Chem Eng 2021;99:601–12. https://doi.org/10.1002/cjce.23881.

[51] Gil MV, Martínez M, García S, Rubiera F, Pis JJ, Pevida C. Response surface methodology as an efficient tool for optimizing carbon adsorbents for CO_2 capture. Fuel Process Technol 2013;106:55–61. https://doi.org/10.1016/j.fuproc.2012.06.018.

[52] Tang Q, Lau Y Bin, Hu S, Yan W, Yang Y, Chen T. Response surface methodology using Gaussian processes: Towards optimizing the trans-stilbene epoxidation over Co^{2+}-NaX catalysts. Chem Eng J 2010;156:423–31. https://doi.org/10.1016/j.cej.2009.11.002.

[53] Khajeh M, Ghaemi A. Nanoclay montmorillonite as an adsorbent for CO_2 capture: Experimental and modeling. J Chinese Chem Soc 2020;67:253–66. https://doi.org/10.1002/jccs.201900150.

[54] Amiri M, Shahhosseini S, Ghaemi A. Optimization of CO2 Capture Process from Simulated Flue Gas by Dry Regenerable Alkali Metal Carbonate Based Adsorbent Using Response Surface Methodology. Energy Fuels 2017;31:5286–96. https://doi.org/10.1021/acs.energyfuels.6b03303.

[55] Pashaei H, Ghaemi A, Nasiri M, Karami B. Experimental Modeling and Optimization of CO_2 Absorption into Piperazine Solutions Using RSM-CCD Methodology. ACS Omega 2020;5:8432–48. https://doi.org/10.1021/acsomega.9b03363.

[56] Mourad AAHI, Mohammad AF, Al-Marzouqi AH, El-Naas MH, Al-Marzouqi MH, Altarawneh M, 2022. CO_2 capture and ions removal through reaction with potassium hydroxide in desalination reject brine: Statistical optimization. Chem Eng Process: Process Intensif. 170, 108722. https://doi.org/10.1016/j.cep.2021.108722.

[57] Saeidi M, Ghaemi A, Tahvildari K, Derakhshi P. Exploiting response surface methodology (RSM) as a novel approach for the optimization of carbon dioxide adsorption by dry sodium hydroxide. J Chinese Chem Soc 2018;65:1465–75. https://doi.org/10.1002/jccs.201800012.

[58] Das D, Meikap BC. Optimization of process condition for the preparation of amine-impregnated activated carbon developed for CO_2 capture and applied to methylene blue

adsorption by response surface methodology. J Environ Sci Health 2017;52:1164-72. https://doi.org/10.1080/10934529.2017.1356204.

[59] Song C, Kitamura Y, Li S. Optimization of a novel cryogenic CO_2 capture process by response surface methodology (RSM). J Taiwan Inst Chem Eng 2014;45:1666–76. https://doi.org/10.1016/j.jtice.2013.12.009.

[60] Sahraie S, Rashidi H, Valeh-e-Sheyda P. An optimization framework to investigate the CO_2 capture performance by MEA: Experimental and statistical studies using Box-Behnken design. Process Saf Environ Prot 2019;122:161-8. https://doi.org/10.1016/j.psep.2018.11.026.

[61] Nuchitprasittichai A, Cremaschi S. Optimization of CO_2 capture process with aqueous amines using response surface methodology. Comput Chem Eng 2011;35:1521–31. https://doi.org/10.1016/j.compchemeng.2011.03.016.

[62] Nuchitprasittichai A, Cremaschi S. Optimization of CO_2 Capture Process with Aqueous Amines - A Comparison of Two Simulation – Optimization Approaches. Ind Eng Chem Res 2013;52:10236-43. https://doi.org/10.1021/ie3029366.

[63] Rho SW, Yoo KP, Lee JS, Nam SC, Son JE, Min BM. Solubility of CO_2 in aqueous methyldiethanolamine solutions. J Chem Eng Data 1997;42:1161–4. https://doi.org/10.1021/je970097d.

[64] Kim I, Svendsen HF. Heat of absorption of carbon dioxide (CO_2) in monoethanolamine (MEA) and 2-(aminoethyl)ethanolamine (AEEA) solutions. Ind Eng Chem Res 2007;46:5803–9. https://doi.org/10.1021/ie0616489.

[65] Mathias PM, O'Connell JP. The Gibbs-Helmholtz equation and the thermodynamic consistency of chemical absorption data. Ind Eng Chem Res 2012;51:5090–7. https://doi.org/10.1021/ie202668k.

[66] Caplow M. Kinetics of Carbamate Formation and Breakdown. J Am Chem Soc 1968;90:6795–803. https://doi.org/10.1021/ja01026a041.

[67 Danckwerts PV. The reaction of CO_2 with ethanolamines. Chem Eng Sci 1979;34:443–6. https://doi.org/10.1016/0009-2509(79)85087-3.

[68] Donaldson TL, Nguyen YN. Carbon Dioxide Reaction Kinetics and Transport in Aqueous Amine Membranes. Ind Eng Chem Fundam 1980;19:260–6. https://doi.org/10.1021/i160075a005.

[69] Perinu C, Arstad B, Jens KJ. NMR spectroscopy applied to amine–CO_2–H_2O systems relevant for post-combustion CO_2 capture: A review. Int J Greenh Gas Control 2014;20:230-43. https://doi.org/10.1016/j.ijggc.2013.10.029.

[70] Lee JI, Otto FD, Mather AE. Equilibrium Between Carbon Dioxide and Aqueous Monoethanolamine Solutions. J Appl Chem Biotechnol 1976;26:541–9. https://doi.org/10.1002/jctb.5020260177.

[71] Shen KP, Li MH. Solubility of carbon dioxide in aqueous mixtures of monoethanolamine with methyldiethanolamine. J Chem Eng Data 1992;37:96-100. https://doi.org/10.1021/je00005a025.

[72] Tong D, Trusler JM, Maitland GC, Gibbins J, Fennell PS. Solubility of carbon dioxide in aqueous solution of monoethanolamine or 2-amino-2-methyl-1-propanol: Experimental measurements and modeling. Int J Greenh Gas Control 2012;6:37-47. https://doi.org/10.1016/j.ijggc.2011.11.005.

[73] Gao H, Wu Z, Liu H, Luo X, Liang Z. Experimental Studies on the Effect of Tertiary Amine Promoters in Aqueous Monoethanolamine (MEA) Solutions on the Absorption/Stripping Performances in Post-combustion CO_2 Capture. Energy Fuels 2017;31:13883-91. https://doi.org/10.1021/acs.energyfuels.7b02390.

[74] Im J, Hong SY, Cheon Y, Lee J, Lee JS, Kim HS, et al. Steric hindrance-induced zwitterionic carbonates from alkanolamines and CO_2: Highly efficient CO_2 absorbents. Energy Environ Sci 2011;4:4284–9.https://doi.org/10.1039/C1EE01801A.

[75] Agnihotri N, Mondal MK, 2023. Process parameter variation of Melia azedarach sawdust pyrolysis for fuel properties, physicochemical characterization, and in-depth speciation analysis. Biomass Conv Bioref. https://doi.org/10.1007/s13399-023-04305-7.

[76] Wang X, Zheng K, Peng Z, Liu B, Jia X, Tian J, 2022. Exploiting proton masking to protect amino achieve efficient capture CO_2 by amino-acids deep eutectic solvents. Sep Purif Technol 299, 121787. https://doi.org/10.1016/j.seppur.2022.121787.

[77] Ohno K, Matsumoto H, Yoshida H, Matsuura H, Iwaki T, Suda T. Vibrational Spectroscopic and ab Initio Studies on Conformations of the Chemical Species in a Reaction of Aqueous 2-(N, N-Dimethylamino) ethanol Solutions with Carbon Dioxide. Importance of Strong NH^+...O Hydrogen Bonding. J Phys Chem A. 1998;102:8056–62. https://doi.org/10.1021/jp982562z.

[78] Kortunov PV, Siskin M, Baugh LS, Calabro DC. In Situ Nuclear Magnetic Resonance Mechanistic Studies of Carbon Dioxide Reactions with Liquid Amines in Aqueous Systems: New Insights on Carbon Capture Reaction Pathways. Energy Fuels 2015;29:5919–39. https://doi.org/10.1021/acs.energyfuels.5b00850.

[79] https://www.fishersci.com/store/msds?partNumber=AC126720010&productDescription=N-METHYLDIETHANOLAMINE%2C+1KG&vendorId=VN00032119&countryCode=US&language=en (accessed 02 February 2023).

[80] Spectrum. https://www.spectrumchemical.com/media/sds/AM156_AGHS.pdf (accessed 02 February 2023).

[81] Ted Pella. https://www.tedpella.com/SDS_html/18315_sds.pdf (accessed 02 February 2023).

[82] Oxford Lab Fine. https://www.oxfordlabchem.com/msds/PIPERAZINE%20(Anhydrous)._pdf (accessed 02 February).

[83] Alliance Chemicals. https://www.alliancechemicals.com/wp-content/uploads/2011/10/DEA-sds.pdf (accessed 02 February).

[84] North Metal and Chemical. https://northmetal.net/wp-content/uploads/Diethylaminoethanol-Diethylethanolamine-DEAE-DEEA-Pennad-150-C6H15NO-100-37-8-SDS.pdf (accessed 02 February).

[85] Alliance Chemicals. https://www.alliancechemicals.com/wp-content/uploads/2019/01/MEA- sds.pdf (accessed 02 February).

[86] Merck. https://www.sigmaaldrich.com/IN/en/sds/aldrich/471496 (accessed 02 February).

[87] Hemmati A, Rashidi H, Hemmati A, Kazemi A. Using rate based simulation, sensitivity analysis and response surface methodology for optimization of an industrial CO_2

capture plant. J Nat Gas Sci Eng 2019;62:101-12. https://doi.org/10.1016/j.jngse.2018.12.002.

[88] Garcia S, Gil MV, Martín CF, Pis JJ, Rubiera F, Pevida C. Breakthrough adsorption study of a commercial activated carbon for pre-combustion CO_2 capture. Chem Eng J 2011;171:549-56. https://doi.org/10.1016/j.cej.2011.04.027.

[89] Shafeeyan MS, Daud WM, Houshmand A, Arami-Niya A. The application of response surface methodology to optimize the amination of activated carbon for the preparation of carbon dioxide adsorbents. Fuel 2012;94:465-72. https://doi.org/10.1016/j.fuel.2011.11.035.

[90] Gupta AK, Gautam A, Mondal MK. Experimental, modeling and RSM optimization of CO_2 loading for an aqueous blend of diethylenetriamine and 3-dimethyl amino-1-propanol. Korean J Chem Eng 2023;40:1151-67. https://doi.org/10.1007/s11814-022-1300-3